Climate Dynamics
https://doi.org/10.1007/s00382-021-06053-8

Effects of spring Tibetan Plateau land temperature anomalies on early summer floods/droughts over the monsoon regions of South East Asia

Ismaila Diallo[1] · Yongkang Xue[1,2] · Qiuyu Chen[3] · Xuejuan Ren[3] · Weidong Guo[4]

Received: 28 April 2021 / Accepted: 11 November 2021

Abstract

Recent observational and modeling studies have demonstrated the substantial influence of the Tibetan Plateau (TP) spring land surface temperature (LST) and subsurface temperature (SUBT) on downstream summer droughts/floods events in East Asia, highlighting the potential application of LST/SUBT on sub-seasonal to seasonal prediction (S2S). In this study, we employ the National Centers for Environment Prediction—Global Forecast System/Simplified Simple Biosphere model version 2 (GFS/SSiB2) to investigate the potential role of the late spring warm LST anomaly over the TP on the extraordinary June 1998 flood in the south of the Yangtze River region. Numerical experiments indicate that the warmer (above normal) May LST over the TP may contribute to the extreme flood of 1998 over the south of the Yangtze River region, with the LST reproducing about 57% and 64% of observed above-normal rainfall anomaly over the south of the Yangtze River region and southeastern China, respectively. Further analyses reveal a possible effect of springtime TP's LST on summer southern and eastern Asian rainfall and identify some hot spots, suggesting that the TP's spring LST effect is not only limited to the Yangtze River region, but to a much larger scale. The imposed warm LST/SUBT over the TP triggers a strong wave activities propagating eastward along the upper-level westerly jet, associated with an increase of the atmospheric baroclinic instability as well as a strengthening and southeastward movement of the South Asian high, leading to intensified moisture convergence and convective instability favorable to the excessive rainfall in the downstream region of East Asia. The results of the 1998 case have also been compared with the results from year of 2003, which had a very cold spring LST anomaly over the TP and a severe downstream June 2003 drought (flood) in southern (northern) of the Yangtze River Basin area. Simulation results provide further evidence of the great importance of the TP spring land surface temperature anomaly in regulating summer extreme hydroclimatic events (e.g. droughts and floods) in South and East Asia. The present study suggests that consideration of LST/SUBT anomalies has a strong potential for more skillful S2S prediction of extreme hydroclimatic events such as floods, droughts and heatwaves over both Southern and Eastern Asia.

Keywords Land surface temperature and subsurface temperature (LST/SUBT) · Tibetan Plateau (TP) · Floods/droughts · East Asian and South Asian summer monsoon · South Asian high · Sub-seasonal to seasonal (S2S) predictability

1 Introduction

Asian summer monsoon rainfall exhibits significant interannual variability, which frequently promotes severe drought or disastrous flood throughout East Asia and South Asia, along with impacts on the social and economic development of the region (Wang 2006; Huang et al. 2007; Zhang and Zhou 2015). For instance, in June 1998 occurs around the Yangtze River Basin/valley of China (hereafter YRB) one of the most disastrous flood on record that the region has witnessed over the last half century, leading to high death toll (more than 3000 people dead), social losses, and material damage (Jiang et al. 2008a, b). The Great Flood of 1998

✉ Ismaila Diallo
idiallo.work@gmail.com; ismailladiallo@gmail.com

1 Department of Geography, University of California, Los Angeles (UCLA), Los Angeles, CA 90095-1524, USA

2 Department of Atmospheric and Oceanic Sciences, UCLA, Los Angeles, CA 90095-1524, USA

3 CMA-NJU Joint Laboratory for Climate Prediction Studies, Institute for Climate and Global Change Research, School of Atmospheric Science, Nanjing University, Nanjing, China

4 Institute for Climate and Global Change Research, School of Atmospheric Sciences, Nanjing University, Nanjing 210023, China

Published online: 08 January 2022

along the YRB region was indeed the largest flood since 1954 (China Meteorological Administration [CMA] 1999). The heavy rain caused numerous and frequent flood peaks in the Yangtze River, and led to a prolonged extreme flood period that lasted for several consecutive weeks (Jiang et al. 2008a, b). Such wide range and long duration of the rainstorm and extreme flood that occurred in 1998 were rare in history and turned out to be the worldwide ever costliest flood event, with direct economic damage of 260 billion Chinese Yuan (i.e., about 31 billion US dollars) (Huang et al. 1998; Lu 2000; Ministry of Water Resources of China 1999; Jiang et al. 2008a, b and references therein).

In addition to flood, droughts also occurred in this region. Local agriculture, socioeconomic development, and ecosystems have been severely jeopardized by droughts (Zhang and Zhou 2015). The 2003 summer season was characterized by a severe drought and abnormal heat over the southern part of the YRB region in eastern China. The extreme heat and continuous drought in 2003 over the southern part of YRB caused serious crop disaster and greatly affected life and production of the society (CMA 2004), which resulted to an economic loss of 5.8 billion Chinese Yuan along with grain losses of about $20–25 \times 10^9$ kg (Zhang and Zhou 2015). This heat event was considered to be an episode of strong interannual variability (Wang et al. 2006). It is therefore imperative for a better understanding and more skillful prediction of hydroclimatic extreme events, in order to provide insight into the potential impact of different mitigation policies.

Many factors may contribute to the variability and spatial distribution of the East Asian summer monsoon rainfall such as sea surface temperature (SST) anomalies in the tropical Pacific ocean, the north Atlantic Ocean and the tropical Indian Ocean, increased anthropogenic aerosol levels, global warming, and land-sea thermal contrast (Yanai and Wu 2006; Wu et al. 2012; Li et al. 2010; Zuo et al. 2013; Duan et al. 2011; Xu et al. 2015; Takaya et al. 2020; among others). For instance, in the tropics the strongly coupled sea-air interactions, known as the El Nino-Southern Oscillation (ENSO) is well correlated with this variability (e.g., Tian and Yasunari 1992; Wang et al. 2000; Lau and Weng 2001; Wu et al. 2003, among others). In addition, the Pacific Decadal Oscillation phase shift exerts a strengthened impact on the eastern China recent decadal summer rainfall variation (Chen et al. 2019). Recently, Zhou et al. (2021) conclude that the late 2019 strong Indian Ocean Dipole was an important contributor to the 2020 extreme Yangtze River flooding. Choi and Ahn (2019) report that cold (warm) tropical SST during May is followed by a weak (strong) East Asian summer monsoon with negative (positive) precipitation anomalies over the South East Asia. Other studies found that the summer monsoon rainfall variability there is associated with a north–south circulation oscillation called the Pacific-Japan pattern and suggested that this pattern is forced by the anomalous SST in the tropical Western Pacific (Nitta 1987; Lau 1992; Huang and Sun 1992).

The Tibetan Plateau (TP), the highest and most extensive plateau on Earth with an area of about 2.5 millions km^2 and an average of over 4000 m above sea level, plays an important role in regulating the global and regional climate, and influence across Eurasia the large-scale atmospheric circulation (Duan and Wu 2005; Yao et al. 2019). As the "water tower of Asia", the TP is also called the third pole. In fact, the TP enhances the East Asian summer monsoon system that brought every year abundant precipitation over East Asia, which mainly includes China, Korea Peninsula, Mongolia, and Japan (Zhisheng et al. 2001; Liu and Yin 2002; Jiang et al. 2008a, b; Zhou et al. 2021). Likewise, the TP causes two main influences: the topographic effect and its thermal effect (Duan and Wu 2005). Without the TP, the South Asian monsoon would be much weaker than the present day, while the precipitation over East Asia would be decreased (Jiang et al. 2008a, b; Wang et al. 2017; Asfhaq 2020). Numerical studies suggest both the TP surface sensible heat flux (Liu et al. 2012; Wang et al. 2014; Wu and Liu 2016) and soil moisture (Xue et al. 2004; Chow et al. 2008; Wan et al. 2017; Gao et al. 2020; Ullah et al 2021, among others) contribute to regulate the summer rainfall in East Asia. While it has also been suggested that the TP heating effect might affect the East Asian summer monsoon rainfall, numerous studies have documented the relationship between snow cover in the TP and both the Indian and Asian summer monsoon variability (Dey and Kumar 1983; Bamzai and Shukla 1999; Kripalani et al. 2003; Wu and Qian 2003; Fasullo 2004). But some studies have found difficulty in using directly the TP snow cover as a predictor for both South and East Asian flood/drought events. Substantial efforts have been undertaken to understand the sensitivity of intra-seasonal and interannual precipitation variability to the TP land surface warming (Li and Yanai 1996; Duan and Wu 2005; Liu et al. 2012; Wang et al. 2014). However, there has been less attention paid to the potential impact of the TP springtime land surface temperature anomaly on the summer East Asian and South Asian hydroclimatic events, such as droughts, floods, and heatwaves.

Using observation and numerical modeling datasets, preliminary studies (Xue et al. 2012, 2016a, b, 2018; Diallo et al. 2019) have shown a significant relationship between the spring land surface temperature (LST) anomaly over the western North America (hereafter western U.S.)/Tibetan Plateau (TP) and the downstream boreal late spring/summer precipitation anomaly over the Southern Great Plain (SGP)/East China. Nowadays, it has been established that the spring subsurface soil temperature (SUBT) and LST anomalies over the western North America play substantial roles in controlling the summer hydroclimatic regime variability over the SGP. Using an

atmospheric Global Climate Model (GCM) and a Regional Climate Model (RCM), Xue et al. (2016a, b, 2018) have investigated the potential contribution of the spring western North America LST/SUBT anomalies to the unprecedented 2011 summer SGP drought/2015 early summer flood and have found that the 2011/2015 cool/warm western North America LST/SUBT anomalies were able to simulate/reproduce about 30% and 34% of the observed 2011 SGP subsequent drought and abnormal heat, and 34% of observed above normal rainfall for 2015, respectively. The 2m air temperature (T-2m) has a substantial global coverage, and early studies have found that its values are very comparable to the LST in stations with measurements for both (Good et al. 2017; Liu et al. 2020; Xue et al. 2021; among others). Because of the promising results, from the use of the springtime 2m-temperature (LST) anomaly for sub-seasonal to seasonal prediction (S2S), a multi-model framework under the Global Energy and Water Exchanges project (GEWEX) and the Third Pole Environment (TPE) support has been initiated to further investigate and explore the impact of initialized LST and snowpack on sub-seasonal to seasonal prediction (LS4P; https://ls4p.geog.ucla.edu/) (Xue et al. 2021).

However, for the East Asia, only one 2003 case with a cold spring TP LST anomaly was investigated (Xue et al. 2018, 2021), but still, no study has comprehensively investigated and elucidated the potential mechanisms of LST and SUBT effects in East Asia. To further examine the TP spring LST effect, along with explore and elucidate its mechanisms, more case studies are necessary. In this study using the National Centers for Environment Prediction—Global Forecast System coupled to the Simplified Simple Biosphere model version 2 vegetation biophysical process model as land surface models, (hereafter, GFS/SSiB2; Xue et al. 2004; Lee et al. 2019), we will investigate the extent to which the warm springtime LST/SUBT across the TP has influenced the 1998 East Asian disastrous flood. The results of the 1998 case will also be compared with the results from year of 2003, which had a very cold spring LST anomaly over the TP. Lastly, we will explore and propose possible mechanisms and associated physical processes through which the spring Tibetan Plateau LST and SUBT affect summer downstream rainfall anomaly in East Asia.

The paper is organized as follows. Section 2 describes the model configurations and different experimental designs as well as the methodology adopted and the reference datasets used for validation and comparisons. Results and discussions are presented in Sect. 3, where the evaluation of the Case 1998 CTRL (CTRL98) and the potential role of the TP spring LST/SUBT on June 1998 south of the Yangtze River region extreme flood are examined, afterward possible mechanisms are elucidated and provided. The results from Case 1998 are also compared with that from a cold spring TP. Finally, the important results obtained in this study are given in the summary and concluding Sect. 4.

2 Observation datasets, model description and experiment design

2.1 Observational data

In this paper, we use the monthly ground-based precipitation and 2m-temperature datasets (http://data.cma.cn/data/cdcdetail/dataCode/SURF_CLI_CHN_PRE_DAY_GRID_0.5.html) provided by the China Meteorological Administration (CMA; V2.0) with a regular horizontal grid-spacing of 0.5° latitude by 0.5° longitude (Han et al. 2019). These datasets are compiled by the National Meteorological Information Center (NMIC) of the CMA (Zhang et al. 2016) and cover the period from 1980 to 2013. The CMA datasets are collected from more than 2400 stations over the entire mainland China and have been interpolated to regular latitude–longitude grids using Thin Plate Spline algorithm based on an "anomaly approach" (Wu and Gao 2013). Indeed, CMA gridded datasets are highly reliable and currently the best available high resolution large-scale near-ground temperature (i.e. land surface temperature [LST] or 2m-temperature [T2m]) and precipitation datasets for the mainland China (Ren et al. 2015a, b; Han et al. 2019; Xue et al. 2021).

In addition, we utilize the monthly gridded precipitation datasets obtained from the latest version of the Climate Research Unit gridded Time Series version 4 (CRUTS v4; Harris et al. 2020) at the University of East Anglia. CRUTS v4 (hereafter CRU) is a widely used climate datasets available from 1901 to 2018. These time-series datasets are calculated on a high-resolution of 0.5° latitude by 0.5° longitude grids over all land domains of the world (except for Antarctica). For China, the monthly mean rainfall from the aforementioned two products (CMA and CRU) presents a good agreement for interannual variability, intra-seasonal variability, spatial distribution and annual cycle with a high correlation between the two datasets (Zhao and Fu 2006; You et al. 2015). For near surface temperature, we also used the second version of Global Historical Climatology Network and the Climate Anomaly Monitoring System (GHCN_CAMS, hereafter CAMS) gauge-based 2m-temperature (Fan and van den Dool 2008). With a regular horizontal resolution of 0.5° longitude × 0.5° latitude grids, CAMS provides monthly mean global coverage over land from 1948 to near present. Despite a good agreement for 2m-temperature spatial distribution and temporal evolution between CAMS and CMA over China, over the Tibetan Plateau (TP) the May near surface temperature climatology (1980–2013 average) for CAMS is about 1.8 °C cooler than CMA climatology (Xue et al. 2021). But, compared with the CMA data, the mean absolute

bias of CAMS/CRU 2m-temperature climatology over the TP for May is 0.1/0.8 °C warmer, respectively (not shown).

For the monthly atmospheric fields including air temperature, geopotential height and horizontal wind, we utilize the National Aeronautics and Space Administration (NASA) Modern-Era Retrospective Analysis for Research and Application version 2 (MERRA-2; Gelaro et al. 2017) reanalysis datasets. This datasets have a horizontal resolution of 0.5° latitude × 0.625° longitude with 72 pressure levels, and cover the period from 1979 to the near present. Likewise, similar large-scale atmospheric circulation variables datasets derived from the National Centers for Environmental Prediction-National Center for Atmospheric Research reanalysis (NCEP-NCAR; Kalnay et al. 1996) on a 2.5° longitude × 2.5° latitude grid-point basis with 17 pressure levels and covering the period from 1979 to near present, are also used. Similarly to Diallo et al. (2019), in this study the anomaly from observations and/or reanalysis refers to the departure relative to the climatology of 1981–2010.

2.2 Model description

In this study, we adopt the National Centre for Environmental Prediction—Global Forecast System (NCEP-GFS) from the version 2 of the NCEP Climate Forecast System (CFSv2) model (Kanamitsu et al. 2002; Saha et al. 2014). NCEP-GFS is a state-of-the-art global atmospheric model used for seasonal and sub-seasonal monsoon prediction. We set the NCEP-GFS spectral discretization at T126 L64, which has a horizontal grid-spacing of about 100 × 100 km and 64 vertical levels with most located in the troposphere. T126 corresponds to equally spaced grid points over 384 longitudes and 190 latitudes, with a horizontal resolution of about 1° latitude by 1° longitude grids at the equator. The NCEP-GFS selected parameterizations and physics include: (1) a convective gravity wave drag based from the theory of Chun and Baik (1998), (2) a non-local scheme for the boundary layer vertical diffusion (Hong and Pan 1996), (3) a modified version of the Simplified Arakawa-Schubert (SAS) for the mass-flux shallow convection and cumulus convection (Arakawa and Schubert 1974; Pan and Wu 1995; Hong and Pan 1998), (4) the cloud microphysical processes (except for auto-conversion) of Zhao and Carr (1997) updated by Moorthi et al. (2001) to determine the prognostic cloud water and ice mixing ratios, and (5) the Rapid Radiative Transfert Models from Atmospheric and Environmental Research (Pincus et al. 2003; Mlawer et al. 1997; Clough et al. 2005) for shortwave and longwave radiation. The second generation of the Simplified Simple Biosphere biophysical model (SSiB2) is coupled with the NCEP-GFS as the land surface model for the representation of land surface processes (Xue et al. 1991; Zhan et al. 2003; Diallo et al. 2019; hereafter GFS/SSiB2). Further detailed description of the GFS/SSiB2 parameterizations, along with its performances to simulate various aspects of the mean climate and associated large-scale circulation characteristics can be found in Lee et al. (2019) and Diallo et al. (2019).

The SSiB2 is a state-of-the-art vegetation biophysical model including 13 vegetation-cover types, with one vegetation type per grid cell. It has one vegetation layer and three soil layers, whilst the vegetation type includes grassland, tropical forest, crop land, shrubs, mixed broadleaf and needleleaf tree (Xue et al. 2004). Dickinson's (1988) revised force-restore method was employed to represent and/or calculate the heat transfer between the surface and subsurface soil layers in SSiB2. At the atmosphere-land interface, SSiB2 preserves energy, water, and momentum conservation, while considering explicitly the water and energy exchanges between the atmosphere and the land (Xue et al. 1991; Sellers et al. 1996; Zhan et al. 2003).

2.3 Background: observed relationship

The significant relationship between springtime land surface temperature (LST) and subsurface temperature (SUBT) anomalies over high mountain areas over the western North America/Tibetan Plateau and summer downstream precipitation anomaly in North America/East Asia has been reported in recent research (Xue et al. 2012, 2016a, b, 2018; Diallo et al. 2019). In this section, we use CMA observations to further discuss the observational relationship between near surface temperature and precipitation in East Asia, as well as to underpin the experimental design in this study. For convenience, in this paper the regionally averaged 2m-temperature for May over the TP where topography is higher than 4000 m is referred to as the TP-LST. Figure 1a displays the spatial distribution of the June climatological (here, we used the 1980–2013) mean precipitation in mainland China. Rainfall greater than 6 mm/day is located in the south of the Yangtze River Basin (YRB) region, with maximum amount exceeding 8 mm/day located along the southern coastal and southeastern areas of the East Asia. Overall, rainfall reduces gradually from the south toward the north and the northwest. Figure 1b displays the corresponding standard deviation of rainfall, showing in southeast China one significant core of rainfall variance, which suggests a strong interannual variability (i.e. year-to-year fluctuations) of the early East Asian summer monsoon rainfall. In contrast, little precipitation variability is observed in the Tibetan Plateau, westernmost, and northeastern China. The area bounded by 107° E–121° E and 22° N–31° N (for reference see blue box in Fig. 1a) shows the maximum rainfall climatology and variance. This domain is referred as the main region of the south of YRB area in this paper, to be later discussed. The year-to-year fluctuation can lead to severe/disastrous droughts/floods in the south of the YRB area, such as the worst (severe) flood

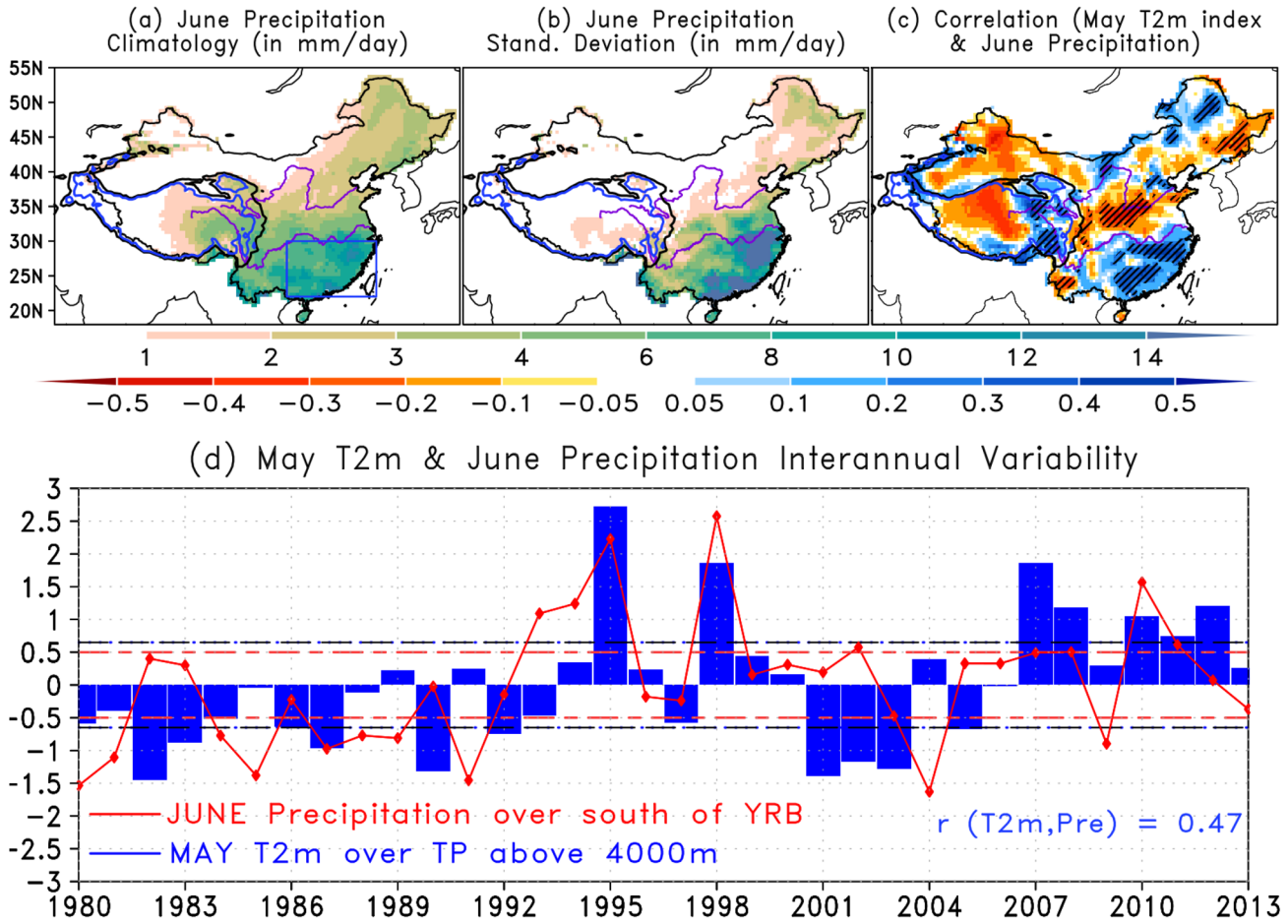

Fig. 1 **a** Spatial pattern of mean mainland China monsoon rainfall (unit: mm/day) in June during 1980–2013. **b** The corresponding variances (units: mm^2/day^2). **c** Interannual spatial correlation coefficient between May 2m-temperature averaged over the Tibetan Plateau above 4000 m and June China monsoon rainfall during 1980–2013. **d** Normalized interannual time series of 2m-temeprature averaged over the TP above 4000 m and June rainfall averaged over the south of Yangtze River region. The dotted regions in **c** denote the statistical significance at the $\alpha < 0.05$ level of two-tailed t-test values. Box in **a** shows the south of Yangtze River region used for the rainfall regional averages. Blue (red) horizontal dashed line in **d** denotes + 1/− 1 (+ 0.6/− 0.6) standard deviation boundaries for June (May) precipitation (2m-temperature)

(drought) event in 1998 (2003), that substantially affect the social, and the population wellbeing as well as the economic development of the region (Wang 2006; Yasunari and Miwa 2006; Seol and Hong 2009; Wang et al. 2014; Xue et al. 2018).

To identify the spatial distribution of June rainfall anomalies associated with the TP-LST, temporal correlation analysis was conducted for the period 1980–2013 (Fig. 1c). The East Asian lowland plain shows a dipole pattern, as shown in previous studies (Xue et al. 2018, 2021). Significant and positives (negatives) correlations prevail over the south (north) of the YRB area, i.e. the correlation map exhibits a south-wetter-north-drier pattern. In addition, negative correlations but not significant appear over the western of the Tibetan Plateau and the northwestern China (Fig. 1c). The correlations are significant and relatively higher in south and north of the YRB region, indicating stronger linkage/relationship to the TP late spring 2m-temperature. In agreement with Xue et al. (2018), our result implies that when the spring land surface temperature over the TP is above (below) normal, a significant positive (negative) rainfall anomaly appears in the south (north) of YRB region, while in the north (south) of the YRB region occurs a significant negative (positive) rainfall anomaly. To quantitatively clarify this relationship, we display in Fig. 1d the interannual variability of the June rainfall regionally averaged over the south of YRB region and May TP-LST for the period 1980–2013. In 1998 (2003) the spring land surface temperature over TP is obviously warmer (cooler) than the climatology, while the June rainfall over south of YRB region is wetter (drier) than the climatology.

Overall, we note a strong co-variability between the May TP-LST and the June rainfall over the south of YRB region with a temporal correlation coefficient of 0.47. This correlation is statistically significant at $\alpha < 0.05$ confidence level by two-tailed student's T-test and is in the same range with the correlation previously published (Xue et al. 2018) but based on a different method. These statistical results confirm the substantial relationship between the spring land surface temperature anomaly over the TP and the summer rainfall anomaly over the downstream region. Here, we intend to conduct various numerical experiments to further investigate and confirm this relationship, as well as to examine and elucidate possible mechanisms that underline such causal relationship. Overall, our observational results, combined with previous modeling results of the effect of LST and SUBT on the East Asian summer drought, impelled us to investigate whether this causal relationship has existed during 1998 when disastrous south of YRB flood occurred with record-warm late springtime (May) 2m-temperature to the TP. It is worth pointing out that early study (Xue et al. 2018) mainly focused on the LST and SUBT effect on downstream East Asian summer rainfall, whilst in this paper we will explore and isolate the possible mechanisms of the LST and SUBT effect in East Asia. To reach this goal numerical modeling study is fundamental.

2.4 Experimental design

To test the potential contribution of the record-warm TP spring LST to the disastrous flood event in June 1998 over the south of YRB region, we utilize the GFS/SSiB2 model to perform two sets of ensemble scenarios simulations under similar initial atmospheric and land surface conditions, sea surface temperature (SST), and sea-ice forcing. In all scenarios cases, the 1998 atmospheric and land surface conditions data from the NCEP Climate Forecast System reanalysis (CFSR; Saha et al. 2010) as well as 1998 observed sea-ice and 1998 global real time SST analysis from NCEP-R2 were used as initial and lower boundary conditions. Observational LST/SUBT measurements over high-elevation such as TP are vital for model validation and initialization of model surface conditions. However, to date we do not have a long-period large-scale SUBT measurement over the TP, but several studies using observational data revealed strong correlation between LST (2m-temperature) and SUBT (Liu et al. 2020; Hu and Feng 2004).

Table 1 summarizes the details about experimental designs as well as the experiments/cases acronyms. In the first scenario case, we imposed the specified warm LST and SUBT anomalies over the TP based on the CMA 2m-temperature difference between May 1998 and the May climatology (here we used the mean of 1981–2010) with some adjustment (Fig. 2a) and aimed to reproduce the observed warm (positive) May 2m-temperature anomaly over the TP. Xue et al. (2021) have presented the approach in initializing the TP LST/SUBT, for brevity the readers are redirected to that study for more details (e.g., equations, different steps, …etc.) about the method. Note, the warm anomalies are imposed only at the first time step of the model integration, and after the anomalies initial imposition both the LST and SUBT will be updated by the model based on its free integration. This scenario serves as control case and is referred to as "CTRL98". Results from the CTRL98 are used to evaluate GFS/SSiB2 performance in simulating 1998 southern Asian and East Asian early summer monsoon. We carried out a second GFS/SSiB2 scenario case, hereafter referred to as "noSUBT98", in which no warm initial LST and SUBT anomalies are imposed, while all other settings, including physics parameterizations as well as surface and atmospheric initial conditions, are kept similar to CTRL98. Each ensemble scenario case has ten members of continuous simulations with no re-initialization of any fields for the different integrations. The ensemble members were initialized at 00z, 21, 22, 23, 24, 25, 26, 27, 28, 29, and 30 April 1998

Table 1 Experiment design, acronyms and definition of the different experiments/cases

Experiments	Initial imposed LST and SUBT over TP for the 1st time step	Descriptions
CTRL98	Imposed warm LST and SUBT anomaly (see Fig. 2a for the anomaly) at the 1st time step	Examines GFS/SSiB2 control performance for 1998 EASM
noSUBT98	No-imposed anomaly at the 1st time step	Estimates effects of warm late spring LST anomaly over the TP on 1998 EASM
CTRL03	Imposed cold LST and SUBT anomaly (see Fig. 3a for the anomaly) at the 1st time step	Examines GFS/SSiB2 control performance for 2003 EASM
noSUBT03	No-imposed anomaly at the 1st time step	Estimate effects of cold late spring LST anomaly over the TP on 2003 EASM
Case 1998	Difference between CTRL98 and noSUBT98 (CTRL98 minus noSUBT98)	Shows differences due to warm LST and SUBT effect for the warm year (year 1998)
Case 2003	Difference between CTRL03 and noSUBT03 (CTRL03 minus noSUBT03)	Shows differences due to cold LST and SUBT effect for the cold year (year 2003)

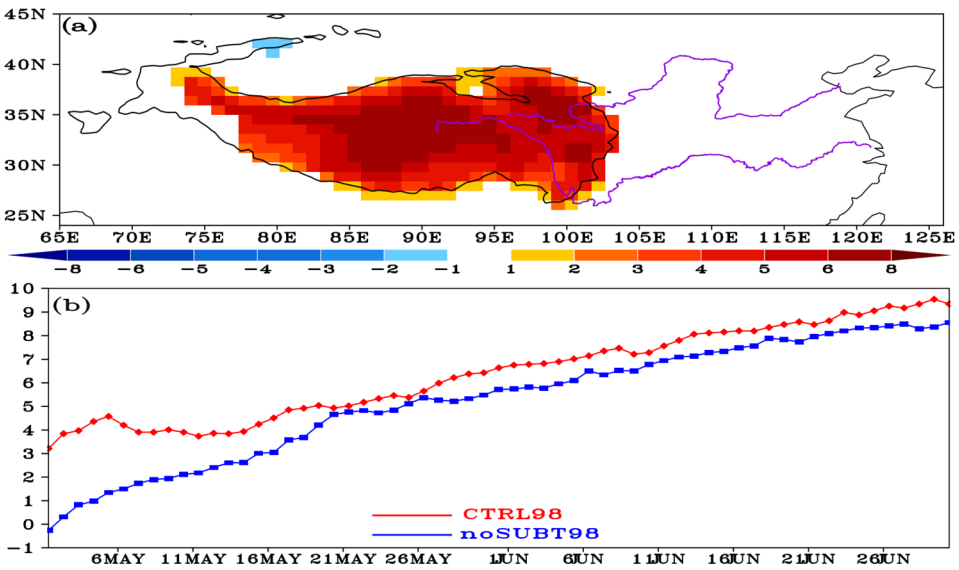

Fig. 2 **a** Imposed sub-surface temperature (SUBT) difference over the Tibetan Plateau at the first time-step of the model simulation between CTRL98 and noSUBT98. **b** Time-series of area-averaged of 2m-temperature (T2m) averaged over the Tibetan Plateau above 4000 m from CTRL98 and noSUBT98. Unit: °C

and ended at 00z 01 July 1998. Note that, all the simulation results presented in this study are based from the multi-member ensemble mean.

Figure 2a displays the initial (first time step) SUBT difference between CTRL98 and noSUBT98, which show warm SUBT over the whole TP with maximum located toward central TP. Despite the larger anomalous magnitude, the SUBT difference shown in Fig. 2a is consistent with the observed 1998 May 2m-temperature anomaly over the TP. Figure 2b presents the evolution of area-average 2m-temperature over TP above 4000 m from the two scenarios experiments. The imposed LST and SUBT lead to a warmer 2m-temperature in CTRL98 which, indeed persisted during the entire integration period, although the warmer anomaly becomes weaker after the third week of May (see Fig. 2b). Note the evolution of 2m-temperature over TP above 4000 m from CTRL98 compares better with the CMA observation (not shown).

To confirm and verify the robustness of the results obtained from the 1998 scenarios study, we conducted another two sets of ensemble scenarios experiments for the year 2003 characterized by a severe/disastrous summer drought/flood over the south/north of the YRB region and cold (below normal) May TP 2m-temperature anomaly (see Fig. 1d). Although this case has been studied in Xue et al. (2018), to compare with the 1998 case, we have rerun the case using similar starting dates with same ensemble member size to the 1998 case, which are more than the ones in Xue et al. (2018). The model initial conditions, parameterization and physics settings used for the 2003 ensemble scenarios experiment are the same as for 1998. In the control scenario case, referred to as "CTRL03", we imposed at the first time step of the model integration the cold LST and SUBT over the TP based on the May 2003 CMA 2m-temperature anomaly, while for the "noSUBT03" experiment scenario (second experiment) no anomalies were imposed over the TP during the entire integration period. Again, each of the ensemble scenario case has ten member ensembles of continuous simulations without re-initialization of any fields for the different period of integrations. The ensemble members were initialized at 00z, 21, 22, 23, 24, 25, 26, 27, 28, 29, and 30 April 2003 and ended at 00z 01 July 2003. The initial SUBT difference between CTRL03 and noSUBT shows cold (negative) SUBT mainly over the TP (Fig. 3a). The imposed anomaly can last more than 40 days (May to early June) and also affects both the sensible heat flux and latent heat flux (Fig. 3b).

Since the difference between CTRL98 (CTRL03) and noSUBT98 (noSUBT03) are mainly attributed to the imposed warm (cold) initial LST/SUBT anomaly at the first time-step (see Table 1 for details), the difference between CTRL98 (CTRL03) and noSUBT98 (noSUBT03) enables us to isolate the potential effect of the LST/SUBT on the June 1998 (2003) extreme flood (severe drought) event over the south of the YRB region. For convenience, here the difference between CTRL98 and noSUBT98 (CTRL98 minus noSUBT98) will henceforth be referred to as Case 1998, while the corresponding difference for the year 2003 (CTRL03 minus noSUBT03) will also be labeled henceforth as Case 2003 (see Table 1). We evaluate the simulated effect of LST/SUBT on rainfall and 2m-temperature from the two cases against observations (CMA/CRU and CMA/CAMS, respectively) anomaly. The CMA, CRU and CAMS anomalies refer in this study to the departures relative to the 1981–2010 climatology periods. Hereinafter "OBS" for the 2m-temperature (precipitation) represents the utilization of CMA (CMA) over mainland China and CAMS (CRU) elsewhere unless specified otherwise.

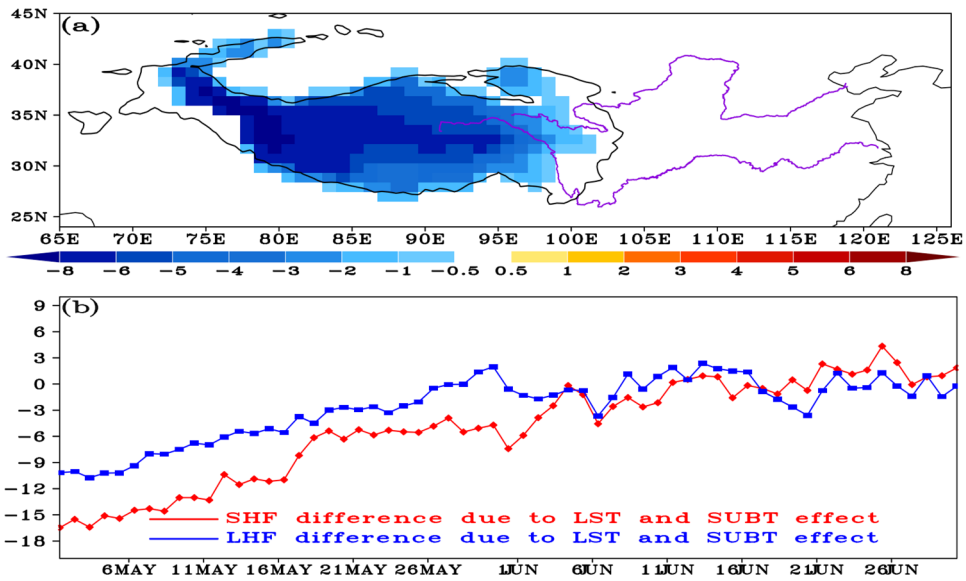

Fig. 3 **a** Imposed sub-surface temperature (SUBT, unit: °C) difference over the Tibetan Plateau at the first time-step of the model simulation between CTRL03 and noSUBT03. **b** Sensible heat flux (SHF, unit: W/m^2) and Latent heat flux (LHF, unit: W/m^2) area-averaged time-series difference between CTRL03 and noSUBT03. The area-averages are performed over the Tibetan Plateau above 4000 m

3 Results and discussion

3.1 Evaluation of CTRL98

The simulation of the Asian Summer Monsoon system, particularly its precipitation and associated large-scale characteristics remain a great challenge for Global Atmospheric Models (Lin et al. 2016; Lee et al. 2019; Lee and Lee 2020; Song and Zhou 2014; among others). In this section, we first evaluate the performance of CTRL98 in simulating the 2m-temperature, precipitation and associated large-scale circulation features for June 1998, before examining the potential impact of the LST and SUBT initialization on the southern Asian and Eastern Asian monsoon. It is worth to note that the simulation for the year of 2003, i.e. CTRL03 has been assessed in Xue et al. (2018) and for brevity will not be presented here, though the two experiments do not have same starting dates and number of member size. Note before computing any statistics, CTRL98 outputs and observations/reanalysis were interpolated to a common $0.5° \times 0.5°$ latitude–longitude grid (i.e., CMA grid) using conservative remapping method (e.g., Diallo et al. 2015, 2018; Anwar and Diallo 2021).

The May 1998 2m-temperature distribution from the OBS and the CTRL98 as well as their corresponding bias distributions are presented in Fig. 4a–c. The OBS shows that the central eastern of the Tibetan Plateau has the lowest temperature (< -3 °C) and the India the highest one (> 33 °C). In China, high 2m-temperature (> 18 °C) can be found in the mid and lower reaches of the Yangtze River valley, Norwest China and South East China, while cold temperature (< 18 °C) are observed in the North West China, Korea, and Japan. CTRL98 reproduces faithfully the overall observed spatial pattern with some discrepancies. In the TP and over the south East China, CTRL98 overestimates the 2m-temperature by about 1 °C, whilst cold biases prevail over both India and the north-eastern Indo China Peninsula (Fig. 4c). To further assess the model performance, different metrics including mean biases (MBs), spatial pattern correlation (PCC), and root mean-square-errors (RMSE) are computed for the TP where topography is higher than both 3000 m and 4000 m (Table 2). 2m-temperature biases with respect to CMA (CAMS) over the TP ranges from 0.64 to 0.87 °C (0.80–1.2 °C) and in most cases spatial correlations exceeds 0.7. Despite some biases/weaknesses, Table 2 and Fig. 4c exhibit that CTRL98 can adequately reproduce the observed 2m-temperature spatial pattern with performance in line with previous application of the GFS/SSiB2 (e.g. Xue et al. 2016a, b, 2018; Lee et al. 2019).

Figure 4d–f shows the June 1998 rainfall from OBS, CTRL98 and their corresponding biases, respectively. Table 2 also synthesizes MB, PCCs, and RMSE of rainfall averaged over the southeastern Asia and the south of the YRB (see boxes in Fig. 4d). OBS shows large amounts of June monsoon rainfall (> 12mm/day) in the South East China (particularly the south of the YRB) and Bangladesh-Myanmar. The June monsoon rainfall in the CTRL98 has a spatial pattern consistent to that of OBS (Fig. 4e), although notable wet/dry biases are also present (Fig. 4f). The rainfall bias over the southeastern China and south of YRB region are -1.26 and -1.92mm/day respectively, while the spatial correlations between CTRL98 and CRU/CMA over both regions exceed 0.67/0.55 (Table 2). The root-mean-square-errors are 3.74 mm/day and 4.40 mm/day, respectively. Furthermore, CTRL98 produces rainfall deficient in India, along the Yangtze River around 28° N, Vietnam and Myanmar, and excess rainfall in the Tibetan Plateau and the coastal of southern China. The largest deficiency over mainland China

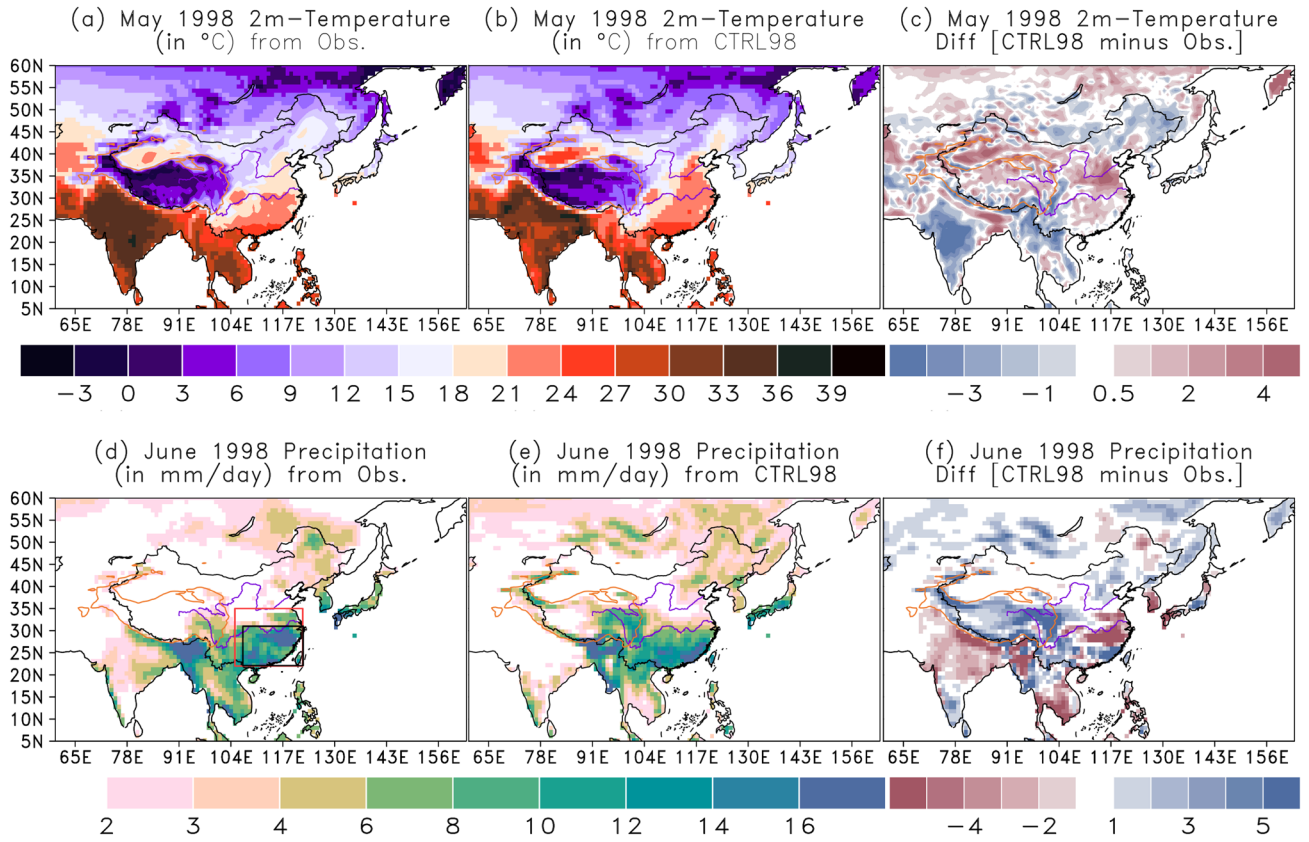

Fig. 4 Mean 2m-temperature for May 1998 (**a**, **b**) and mean biases (**c**). **e**, **f** Same as **a–c** but for June 1998 rainfall. **a** and **d** Observations (OBS), **b** and **e** are GFS/SSiB2 simulations (CTRL98), **c** and **f** are CTRL98 mean biases with respect to observations. Black (red) box in **d** denotes the south of Yangtze River Basin (southeastern China) used for the rainfall regional averages. 2m-temperature (rainfall) unit: °C (mm/day)

Table 2 Mean bias (MB, °C or mm/day), root-mean-square-errors (RMSE, °C or mm/day) and spatial correlation coefficient (PCC) from CTRL98 for 2m-temperature and precipitation in May and June 1998, respectively

Metrics	Tibetan Plateau above 3000 m			Tibetan Plateau above 4000 m		
	MB	RMSE	PCC	MB	RMSE	PCC
2m-Temperature	0.64 (0.80)	2.75 (2.84)	0.72 (0.72)	0.88 (1.20)	2.43 (2.53)	0.71 (0.70)
	South of the Yangtze River (107–122° E and 22–31° N, see black box in Fig. 4d)			Southeastern China (SC, 105–123° E and 22–35° N, see red box in Fig. 4d)		
	MB	RMSE	PCC	MB	RMSE	PCC
Precipitation	− 1.92 (− 1.06)	6.78 (4.40)	0.56 (0.68)	− 1.26 (− 0.74)	5.46 (3.74)	0.61 (0.70)

2m-Temperature metrics are obtained with respect to CMA (CAMS), while those for precipitation are obtained with respect to CMA (CRU)

in CTRL98 is the significant overestimation (underestimation) of rainfall over the TP (along the Yangtze River around 28° N) (Fig. 4f). This could likely be due to the poor representation of fine scale processes and surface heterogeneity in the GFS/SSiB2, owing to its coarse horizontal-resolution. It should be acknowledged that the reason for simulated rainfall bias may also result from other factors (e.g., imperfect large-scale initial conditions, convection parameterization, and cloud microphysics parameterization) which cannot be improved through imposing the LST and SUBT. Lee and Lee (2019) found that the Community Earth System Model version 1.0.4 shows a larger and significant dry bias over south East Asia. However, using the ECHAM6 model, Hertwig et al (2015) show that increasing of their model horizontal resolution results to a reduction of the bias of the simulated mean climate.

Westerly jet streams and subtropical highs play a primary role in the Asian summer monsoon rainfall. Figures 5a–c compare the 200 hPa upper-level mean wind and westerly jet from the NCEP-R2 reanalysis, MERRA2 reanalysis, and CTRL98 for June 1998. The spatial patterns for the upper-level westerly jet in NCEP-R2 and MERRA-2 exhibit a very similar and consistent result with spatial correlation exceeding 0.96 (see Table 3). But with the MERRA-2 reanalysis the core of the westerly jet is stronger and located toward the north. The upper-level wind pattern from both reanalysis and the CTRL98 simulation (Fig. 5a–c) have a remarkable similarity, with the domain spatial correlation coefficients with respect to NCEP-R2/MERRA2 being 0.97/0.95. Although, CTRL98 underestimates the intensity of the westerly jet with the center of the jet slightly shifted toward the east, CTRL98 reproduces reasonably the South Asian high (SAH) as shown and displayed in the 200 hPa anti-cyclonic feature over South Asia and TP.

Figure 5d–f illustrate the 850 hPa lower-level wind vector and air-temperature (shaded) from the two reanalysis datasets and CTRL98, respectively. In South and East Asia, southerly and southwesterly flow prevailed in early summer, i.e. June 1998. CTRL98 replicates realistically the pattern and magnitude of both the low-level wind and air-temperature. However, cold biases are found toward northwest China. Meanwhile, the low-level southwesterly flow passing through eastern China is weaker than in the reanalysis datasets, indicating that CTRL98 simulates lower atmospheric moisture transport. This is consistent with the simulated dry biases over the south of YRB region and southeastern Asia (Fig. 4d–f and Table 3).

In summary, it is found that while CTRL98 simulates warmer bias in May over the Tibetan Plateau, CTRL98 is able to realistically capture the June 1998 southern Asian and east Asian monsoon rainfall band with reasonable

Table 3 Mean bias (MB, units: °C or m/s), root-mean-square-errors (RMSE, units: °C or m/s) and spatial correlation coefficient (PCC) in CTRL98 compared to NCEP-R2 (MERRA2) reanalysis for 200 hPa U-wind and 850 hPa air-temperature in June 1998 over East Asia (60° E–160° E and 5° N–60° N)

	MB	RMSE	PCC
U-Wind at 200 hPa	3.11 (1.14)	5.27 (4.88)	0.97 (0.96)
Air-temperature at 850 hPa	− 1.40 (− 1.12)	2.26 (2.08)	0.95 (0.94)

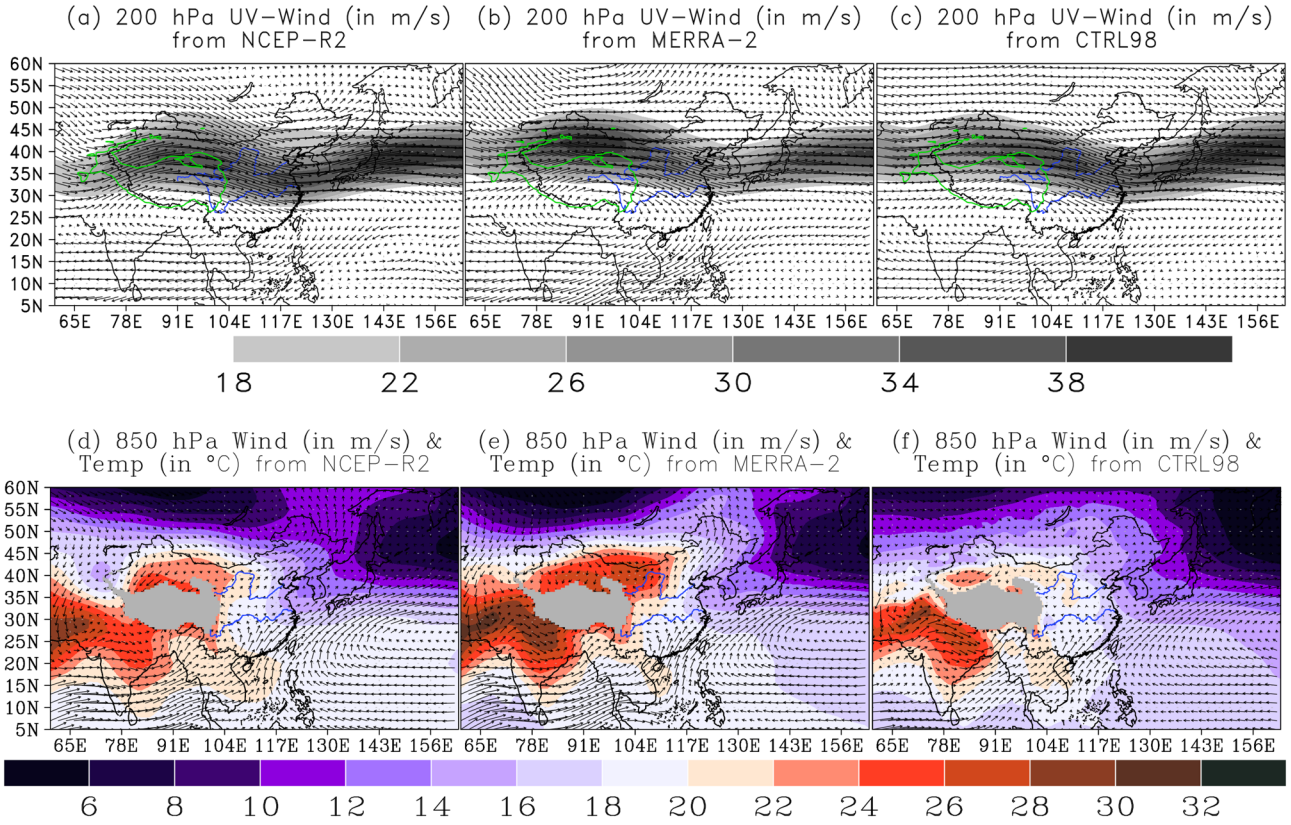

Fig. 5 **a–c** Mean June 1998 of 200 hPa wind vectors (m/s) and the westerly jet (grey shading, m/s) from: **a** NCEP-R2, **b** MERRA-2, and **c** CTRL98. **d–f** same as **a–c**, but for 850 hPa temperature (shading, °C) and low-level wind vectors circulation (m/s). The grey shaded areas in **d–f** denote/highlight the Tibetan Plateau

upper- and low-level large-scale monsoon circulation. These results, indeed, demonstrates that the CTRL98 can simulate the large-scale circulation characteristics, 2m-temperature and rainfall in Asian summer monsoon regions and provides a reasonable basis against which to explore and estimate the potential role of the Tibetan Plateau spring LST and SUBT anomalies on 1998 disastrous early summer floods over East Asia.

3.2 LST and SUBT initialization effect on the 1998 Flood in East Asia

Figure 6a and b displays the 2m-temperature anomalies in May 1998 from OBS and Case 1998, respectively. Note here, that the dots indicate the regions where the differences are statistically significant at $\alpha < 0.05$ confidence levels, as determined by a two-tailed student's t-test. As documented in Sect. 2.4, we imposed the warm LST and SUBT anomalies at the first integration time of the model simulation over the Tibetan Plateau and aimed to reproduce the observed positive May 2m-temperature anomaly over the Tibetan Plateau (Fig. 6a). The OBS displays a positive May temperature anomaly with a magnitude above 1.30 °C over the whole TP, and positive (negative) anomalies in the south (north) of the YRB region. Case 1998 simulates remarkably the extension and magnitude of the 2m-temperature anomaly over the Tibetan Plateau, but does not capture the cold/warm anomalies in the north/south of the Yangtze River valley. Although Case 1998 shows cold/warm bias over the south East China, previous studies have reported that only the 2m-temperature anomaly over high elevations (mountains) had a substantial impact on the extreme summer precipitation in downstream regions in East Asia (Xue et al. 2018) and North America (Xue et al. 2012, 2016a, b, 2018; Diallo et al. 2019). The average 2m-temperature anomalies in May over the TP where topography is higher than 3000/4000 m are 1.42/1.50 °C and 1.04/1.27 °C for OBS and Case 1998, respectively. Consistent with previous studies (Wan et al. 2017; Xue et al. 2021), our results show that from both OBS and simulation, the TP warming rate is larger at higher elevations than at lower elevation. After the Case 1998 reproduces reasonably the observed May 1998 2m-temperature anomaly over the Tibetan Plateau, in the following section we will show that such warm anomaly is an important contributor to the East Asia, particularly southeast China June 1998 severe flood's development.

Figure 6c displays the observed June 1998 rainfall anomaly (difference between June 1998 and the 1981–2010 climatology). The observed precipitation dataset is from CMA over China, while outside mainland China it is from CRU. Note that the observed rainfall anomaly patterns shown in Fig. 6c bears an overall resemblance to the rainfall pattern projected as a consequence of the springtime TP land surface temperature anomaly (see Figs. 1c and 6d). The observed anomaly shows heavy rainfall in the region south of YRB and drought conditions to the north. In addition, wet conditions are observed to the southeastern flank of the TP, while a slightly dry anomaly is located toward the central-west of the TP. Consistent to the observed anomaly, Case 1998 showed that the Tibetan Plateau springtime warm LST and SUBT anomalies produced statistically significant wet June conditions in the area south of the YRB (Fig. 6d). While

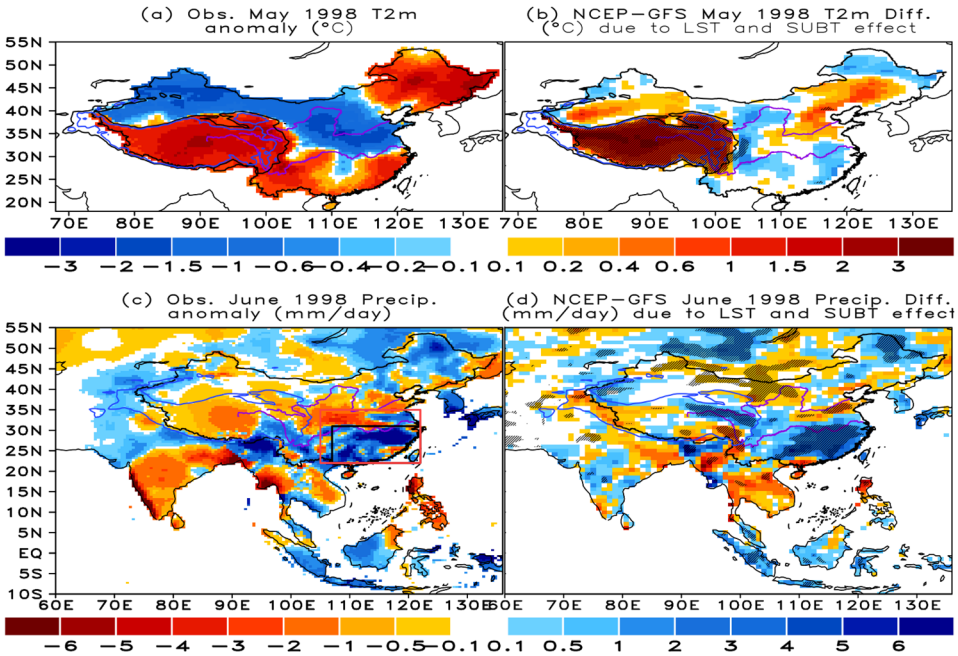

Fig. 6 Observed and simulated May 1998 2m-temperature anomalies (°C). **a** Observed May 2m-T difference between 1998 and the climatology reference (1981–2010); **b** GFS/SSiB2 simulated 2m-T difference due to LST and SUBT effect. **c, d** same as **a, b** but for June 1998 precipitation anomalies (mm/day). Black (red) box in **c** denotes the south of Yangtze River Basin (southeastern China) used for the rainfall regional averages. The dotted regions denote the statistical significance at the $\alpha < 0.05$ level of two-tailed t-test values

there are clear differences in terms of numerical experiment framework between this study and any of the earlier studies except Xue et al. (2018), yet, the simulated downstream East Asian summer rainfall results present some commonalities. Specifically, there were several conceptual studies that imposed (changed) artificially sensible heat flux (soil moisture/albedo/snow cover) over the TP land surface to explore the possible atmospheric response across East Asia. Wan et al. (2017) investigate the impact of the TP land surface heating by changing soil moisture initialization over the TP in the Weather Research and Forecasting (WRF; Skamarock et al. 2008; Diallo et al. 2019; Yu et al. 2021) Model on 10 extreme precipitation events in southeast China. They concluded that a greater heating over the TP surface increases total and extreme rainfall in southeast China, including the south of YRB. Likewise, Wang et al. (2008) reported that an increase by more than 2 °C of TP surface air temperature enhance summer rainfall along the mid-lower reach of the Yangtze River valley. Overall, the rainfall anomaly spatial pattern over the region south of the YRB and neighboring region is indeed consistent with those due to the changes in the Tibetan Plateau surface heating (Liu et al. 2012; Wang et al. 2008; Wan et al. 2017; Ge et al. 2019) and the Tibetan Plateau springtime sensible heat flux (Wang et al. 2014; Wu and Liu 2016), although some notable differences on magnitudes and extensions are evident.

It shall be noted that, the wet rainfall area along the eastern flank of the Tibetan Plateau from the Case 1998 is inconsistent with the observed dry conditions there, additionally; the area with positive rainfall anomaly along the north of YRB region is smaller than observed (Fig. 6c, d). The rainfall increase to the eastern flank of the TP is likely due to the intensification of convection induced by the surface heating of the Tibetan Plateau, which is in agreement with previous studies (Wang et al. 2008; Chow et al. 2008; Wan et al. 2017). Table 4 summarizes the Case 1998 results for rainfall anomalies averaged regionally over the southern Yangtze River and the southeastern China. The LST and SUBT effect produced over the southern Yangtze River and southeastern China about 57% and 64% of observed above-normal rainfall condition, respectively (Table 4), which is consistent with the 62% contribution to the 2003 south of YRB drought reported by Xue et al. (2018). Using the WRF modeling results, Xue et al. (2018) found that the warm (cold) spring LST and SUBT in western North America contributes to about 29% (31%) to observed 2011 (2015) rainfall drought (flood) over the U.S. South Great Plain. In addition to the Yangtze River valley as well as southeastern China, our results suggest that the Tibetan Plateau spring land surface temperature anomaly effect on summer rainfall anomaly is not only limited to the Yangtze River valley and southeastern China but to a much larger remote regions (Fig. 6c, d). We further identify different hot spots over different Asian regions and/or countries. Those regions/countries include: North Eastern region of India, North East China, Bangladesh, Myanmar, Vietnam, Malaysia, Indonesia, North Korea, South Korea and Japan. These hot spots are consistent with those found in Xue et al. (2021), who hypothesized a possible effect of spring Tibetan Plateau's land surface temperature on global summer precipitation over more hot spots.

In summary, our findings suggest that the warm springtime TP LST and SUBT anomaly has played an important role for the persistence and development in June 1998 (early summer) severe flood disasters in the region south of YRB. However, it is worth mentioning that in addition to the LST and SUBT factors, various factors such as Arctic sea-ice (Zhao et al. 2004; Shen et al. 2019), vegetation (Xue et al.

Table 4 Observed anomalies and simulated anomalies highlighting the LST and SUBT effects for May 2m-temperature (Units: °C) and June precipitation (Units: mm/day) for year 1998 and year 2003

2m-temperature				Precipitation			
TP above 3000 m		TP above 4000 m		South of Yangtze River region (107° E–122° E and 22° N–31° N, black box in Fig. 6c)		Southeastern Asia (105° E–122° E and 22° N–35° N, see red box in Fig. 6c)	
Observation	Case 1998	Observation	Case 1998	Observations	Case 1998	Observations	Case 1998
1.42	1.04	1.50	1.27	3.73	2.09	2.36	1.51
2m-temperature				Precipitation			
TP above 3000 m		TP above 4000 m		South of Yangtze River Basin (107° E–122° E and 22° N–28° N, see blue box in Fig. 13c)		North of Yangtze River Basin (107° E–122° E and 31° N–35° N, see black box in Fig. 13c)	
Observation	Case 2003	Observation	Case 2003	Observations	Case 2003	Observations	Case 2003
− 1.22	− 1.14	− 1.52	− 1.42	− 1.52	− 1.18	1.73	1.03

2010; Notaro et al. 2011; Bamba et al. 2018; Lee and Lee 2019; Huang et al. 2020; Yu et al. 2021; among others), sea surface temperature (Wu et al. 2009; Zheng et al. 2016; Xue et al. 2016a, b, 2018; Diallo et al. 2019; Choi and Ahn 2019), atmospheric internal variability (Ding et al. 2010; Song and Zhou 2015), and soil moisture (Koster et al. 2004; Chow et al. 2008; Gao et al. 2020; Ullah et al 2021) may have also played important roles to the devastating floods in June 1998 that occurred in the region south of YRB. Xue et al. (2018) have compared the effects of the LST/SUBT versus the SST on the severe June 2003 southern YRB region drought. They concluded that, unlike from the North America, the TP LST anomaly is a more important contributor to the East Asian rainfall anomaly compared to SST anomalies. However, the relative contribution of the SST to the extreme YRB flooding of 1998 is beyond the scope of the current study and more cases studies are necessary to isolate the contribution of the aforementioned factors.

3.3 Mechanism analyses

In order to understand the downstream rainfall anomalies induced by the warm LST and SUBT initialization over the Tibetan Plateau, we analyze further the anomalous large-scale atmospheric circulation being responsible for rainfall changes. In June 1998, the imposed warming produces in the lower-level an anomalous cyclonic circulation in southern China, while an anomalous anti-cyclonic circulation is formed in northern China (not shown). Such anomalous cyclone and anti-cyclone modulate directly the southern flood-northern drought. Figure 7a shows the Case 1998 moisture flux convergence (shaded) and moisture flux transport (vectors). The moisture flux is integrated between 1000 and 300 hPa. The Bay of Bengal and South China Sea convey most of the moisture supply over the East Asia. As a result of the enhanced southwesterly flow, excessive moisture converges into the southern Yangtze River Basin region. In addition to the moisture excess, there was a clear enhancement of vertical motion over the southern Yangtze River Basin region, which corresponds well to the location of the severe flooding (see Fig. 7c, d).

Figure 7b displays the 500 hPa temperature anomaly. In East Asia, the mid-tropospheric temperature exhibits a "northwest-cool-east-warm pattern" anomaly with the warming extending over the whole south of YRB region. In fact, over the western/eastern Tibetan plateau the imposed LST and SUBT is conductive to water vapor divergence/convergence over the Tibetan Plateau in June 1998 due to the weaker/stronger warming (see Fig. 7b), corresponding to suppressed/enhanced local rainfall. Figure 7c, d presents the horizontal advection of temperature at 500 hPa and the mean vertical velocity (omega) at 500 hPa for Case 1998, respectively. Clearly, in the mid-troposphere, the warm air is transported from the Tibetan Plateau to the downstream (Fig. 7c), which is an important driver of the Meiyu-Baiu rainfall band (also known as changma in Korea and baiu in

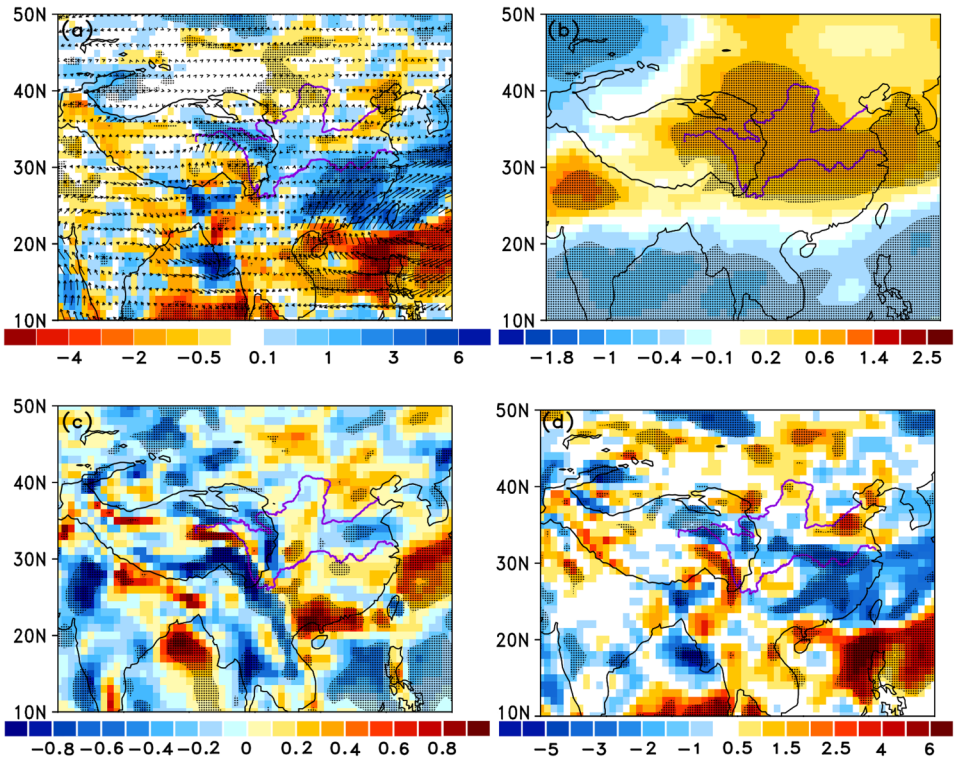

Fig. 7 Simulated June 1998 differences due to LST and SUBT effect for: **a** Vertical integrated (1000–300 hPa) moisture flux transport (vector, kg/m/s) and the corresponding moisture flux convergence (shading, mm/day); **b** 500 hPa air-Temperature (°C); **c** 500 hPa horizontal advection of temperature (units: 10^{-5} K/s); **d** 500 hPa Vertical velocity (unit: 10^{-2} Pa/s). The dotted regions denote the statistical significance at the $\alpha < 0.05$ level of two-tailed t-test values

Japan) (Sampe and Xie 2010; Wang et al 2014). Consistently, the regions of ascending (descending) motions follow closely the region of excess (deficit) rainfall (Figs. 6d and 7d). Furthermore, the imposed warm LST and SUBT induce a prominent correspondence between the warm (cold) advection and rising (sinking) motions in the southern (northern) YRB (Fig. 7c, d). Subsequently, such close correspondence of the horizontal temperature advection with the vertical velocity indicates the crucial role of warm advection for the development of the early summer extreme precipitation in East Asia. More specifically, the warm advection anomaly enhances the upward motion over the southern Yangtze River areas, and as a consequence more rainfall occurs there. Overall, when the Tibetan Plateau late spring 2m-temperture anomaly is warm, both the atmospheric thermodynamic and large-scale dynamic conditions tend to enhance the downstream early summer monsoon rainfall in East Asia.

The consistent results between large-scale circulations and heavy precipitation in the Yangtze River Basin region are the products of the May warm anomaly in TP produced by the imposed warm LST/SUBT at the 1st time-step of the model's integration. The warm anomaly started from the beginning of May and maintained during the whole May (Fig. 8a, b). This warm land surface temperature anomaly produces a positive sensible heat flux anomaly (i.e. an upward flux) and persists in whole May (Fig. 8c, d), which in turn induced a deepening of the planetary boundary layer and the development of a positive anomaly of geopotential height aloft (not shown). It also strengthens over the southern Yangtze River basin a high pressure system and enhances the transport of water vapor from the Bay of Bengal and South China Sea to southern east China (see Fig. 7a). Previous modeling studies have reported the sensitivity of local and remote large scale atmospheric conditions to the Tibetan Plateau surface heating. For instance, in the lower troposphere, the Tibetan Plateau heating generates a cyclonic anomaly, which in turn promotes the intensification of southern China west Pacific subtropical high along with the enhancement of the low-level monsoon jet flow (Wang et al. 2008; Bao et al. 2010; Xiao and Duan 2016). Wan et al (2017) have demonstrated how heating at the TP surface generates a high pressure system downstream, and thereby promotes favorable circulation for heavy precipitation over the south of YRB region. The surface heating anomalies strengthen thermal effect of the Tibetan Plateau then lead to the change of lower atmospheric baroclinicity, which further results in the change of upper atmospheric baroclinicity by the upward spread of baroclinicity wave. The transient eddy activities in the upper troposphere then were changed accordingly (Hoskins 1991; Hsu and Liu 2003; Wang et al. 2008).

The movement of the atmosphere includes zonal mean flow associated with atmospheric circulation and eddy activities. Here we used the eddy kinetic energy (EKE) as an indicator of transient eddy activity energy to show the characteristics of baroclinic wave energy propagation after imposing the warm LST and SUBT anomaly over the Tibetan Plateau. Positive EKE anomaly means stronger wave activities; while negative EKE anomaly indicates weaker wave activities. The formulation of EKE can be written as follow (Wallace et al. 1988; Hoskins and Valdes 1990):

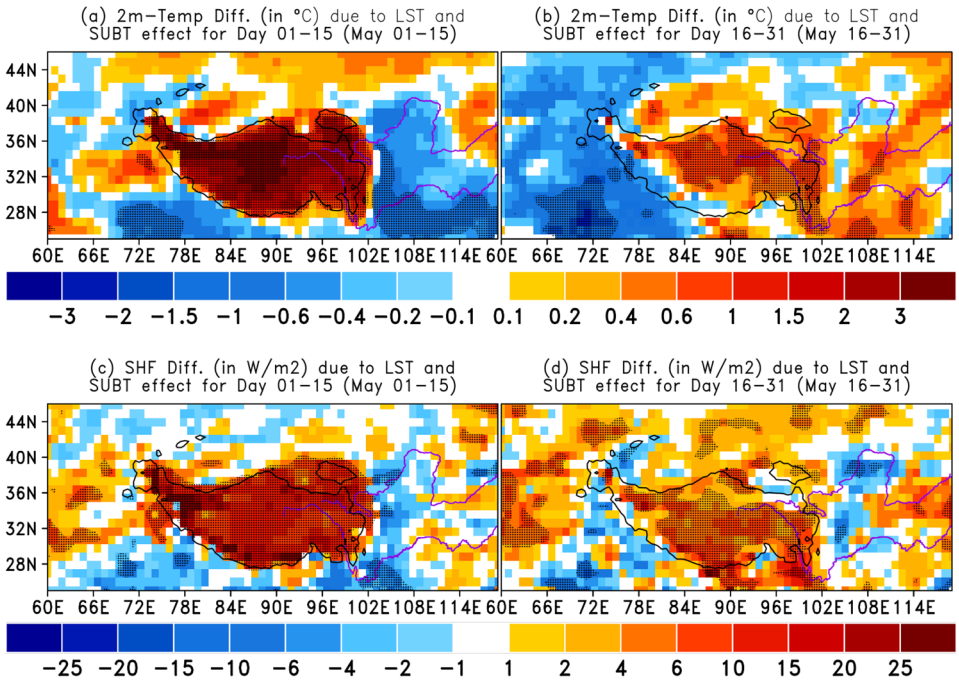

Fig. 8 Simulated 2m-temperature difference (°C) due to LST and SUBT effect for: **a** May 1st–May 15th 1998; **b** May 16th–May 31st 1998. **c, d** Are the same as **a, b** but for the sensible heat flux (SHF, W/m^2). The dotted regions denote the statistical significance at the $\alpha < 0.05$ level of two-tailed t-test values

$$\mathrm{EKE} = \frac{\overline{u'^2} + \overline{v'^2}}{2}$$

where the prime quantity (′) signifies a deviation from the time mean, u', v' are transient disturbance of zonal wind and meridional wind, respectively. The symbol over-bar ("¯") denotes the time average of relative variables. The EKE method has been widely used to investigate the eddy activity, storm tracks and wave flow interactions of the northern hemisphere (Deng and Sun 1994; Vallis and Gerber 2008).

Figure 9a displays the temporal-zonal cross-section of the EKE at 150 hPa averaged within the band 25° N and 35° N, which covers the latitude of the Tibetan Plateau. After the imposed warm anomaly over the Tibetan Plateau, the positive transient eddy anomalies moved eastward indicating the eastward propagation of wave energy during the period of May 1st to May 25th (see Fig. 9a), which in turn leads to the adjustment of waves in the westerlies and further provided energy for the upper-level South Asian high (SAH; also named the Tibetan High) to move eastward (Hoskins and Ambrizzi 1993). Consequently, the SAH shifted eastward during May 1st to May 25th (Fig. 9b). Likewise, the SAH shifted eastward from 90° E to 120° E in May and intensified in June (Fig. 10). The strong wave energy transportation is responsible for the strengthening and eastward movement of the SAH, which are crucial to the excessive heavy precipitation in the south of the YRB. The SAH behavior due to LST and SUBT effect is consistent with the results of Ren et al. (2015a, b) and Ge et al. (2019). Figure 9b also shows that there is a discontinue around May 11th (see core of maximum). This fracture phenomenon commonly exists in the East Asia and North Pacific basin in storm track due to their double-center structure, which is probably associated with the complex location configuration between the westerlies and storm tracks (Deng and Sun 1994; Zhu and Sun 2000).

As a result, the upper level divergence and convergence also changed accordingly. In fact, from May to June, the divergence area extended from the Tibetan Plateau to the southeast China, while the convergence area moved southward and represented a north–south dipole anomaly (Fig. 11a–d). Due to the baroclinic instability of the vertical structure between upper and lower troposphere the divergence and convergence of lower-atmosphere wind field was opposite to the upper troposphere (see Fig. 11 and Fig. S1). Accordingly, excess moisture convergence is developed and sustained in the south of YRB during weeks 3–4 (days 16–30, i.e. May 15–30) and the whole month of June (Fig. 12), leading to extreme flooding along the south of the Yangtze River Basin region. Overall, the imposed warm LST and SUBT anomaly strengthens the Tibetan Plateau diabatic heating and trigger strong wave activities propagating eastward along the upper-level westerly jet, resulting in the strengthening and eastward extension of the SAH, thereby interacting with the upward motion, affecting as a consequence the downstream summer East Asian monsoon rainfall variability.

3.4 LST and SUBT initialization effect on the 2003 Drought in East Asia

In order to verify the robustness of our conclusions for our 1998 case study, we also show some results from the 2003 case and compare it with the 1998 case. The year of 2003 was characterized by a cold spring 2m-temperature anomaly over the Tibetan Plateau and severe/disastrous drought/flood in the southern/northern of the Yangtze River Basin region in June. Figure 13a and b illustrates the 2m-temperature anomalies in May 2003 from OBS and Case 2003, respectively. The observation exhibits a cold (negative) land surface temperature anomaly with a magnitude in the range of − 0.80 to − 1.30 °C over the whole TP, while positive (negative) 2m-temperature anomalies are depicted in the south (north) of the YRB (Fig. 13a). Case 2003 simulates the spatial extension and magnitude of the 2m-temperature anomaly over the Tibetan Plateau, but does not capture the cold anomalies in the south of the YRB and northwest of China (Fig. 13b). The average T-2m anomalies in May over the Tibetan Plateau above 3000/4000 m are − 1.22/− 1.42 °C and − 1.14/− 1.52 °C for OBS and Case 2003, respectively.

Figure 13c presents the observed rainfall anomaly between June 2003 and the climatology, while Table 4 also summarizes the area-averaged rainfall results over the southern and northern Yangtze River basin. Note, to be consistent with the case of year 1998, the figures also include large parts of both southern Asia and eastern Asia. The observed rainfall anomaly shows a severe drought (a reduction of about 1.52mm/day) over the region south of the Yangtze River and wet condition to the north. Case 2003 simulates statistically significant drought/flood conditions over major areas to the south/north of the Yangtze River Basin region (Fig. 13d). However, the wet (dry) conditions to the western flank (central) of the Tibetan Plateau are inconsistent with the observed dry (wet) conditions there. This could likely be due to poor representation of fine-scale processes which are known to influence the skillful simulation of rainfall anomaly due to LST and SUBT effect, particularly over regions with complex topography (Xue et al. 2012; Diallo et al. 2019).

It shall be noted that, in addition to affecting the local and downstream summer climate as addressed in previous study (Xue et al. 2018), this study further identifies that the late springtime cold 2m-temperature anomaly has also a time-lagged impact on the early summer climate in remote regions (see Fig. 13c, d), which is consistent with our Case 1998 study and also speculated in Xue et al. (2021). Consistent to our Case 1998, the Case 2003 results confirm

a possible effect of spring TP's LST on Asian continent summer rainfall with some hot spots identified. Those hot spots include: Japan, northern Indo-China-Peninsula (including Bangladesh, Burma, and northwest Thailand), and South-eastern Asia (see Fig. 13c, d). Nevertheless, it is worth to point out that the previous study focusing on year 2003 (Xue et al. 2018) do not investigate the possible mechanisms responsible for the relationship between the cold spring TP and the June 2003 south-drier-north-wetter pattern anomaly in East Asia. In the next section, we discuss and provide possible mechanisms by which the cold spring TP 2m-temperature impacts summer downstream precipitation in eastern China.

Figure 14a displays the water vapor flux anomalies from Case 2003 integrated vertically from 1000 to 300 hPa in June 2003. We can see that the cold land surface temperature anomaly over the TP in May is conducive to water vapor divergence/convergence over the south/north of YRB, corresponding remarkably with vertical descending/ascending motion (Fig. 14a, b), which is consistent with the rainfall anomaly distribution. Figure 14c shows, as a function of latitude, the vertical cross section of differences for mean vertical motion. Since, we mainly focus on the rainfall over eastern China; the vertical cross-section is averaged from 110° E to 121° E. It can be seen that anomalous descending and ascending motions occur throughout the entire troposphere around 21° N–30° N and 31° N–44° N, respectively. Overall, taken together, cold land surface temperature anomaly over the Tibetan Plateau in May is robustly linked to the water vapor flux divergence/convergence anomalies and anomalous descending (ascending) motion, which provides unfavorable (favorable) dynamics for the summer rainfall over southern (northern) of the YRB. These results provide further evidence of the great importance of the Tibetan Plateau spring land surface temperature anomaly in regulating

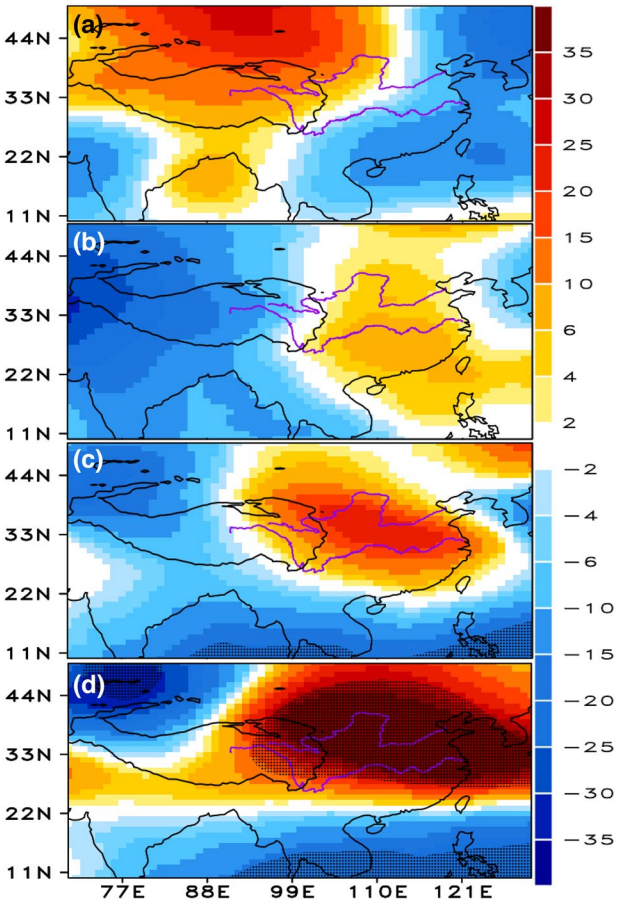

Fig. 10 Difference of geopotential height at 150 hPa (units: m^2/s^2). **a** Day 1–15 (May 1st–May 15th 1998); **b** Day 16–30 (May 16st–May 30th 1998); **c** Day 31–45 (May 31st–June 14th 1998); **d** Day 46–60 (June 15th–June 29th 1998). The dotted regions denote the statistical significance at the $\alpha < 0.05$ level of two-tailed t-test values

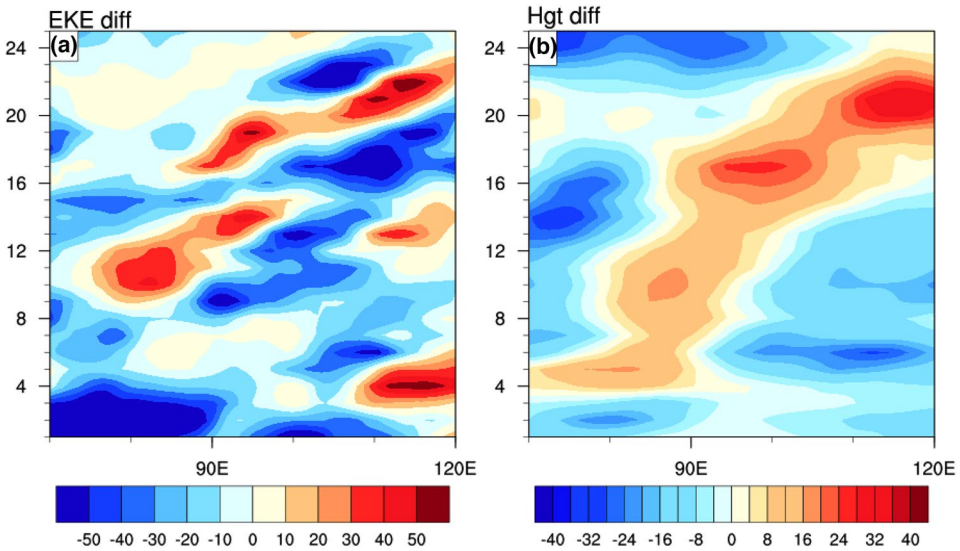

Fig. 9 **a** Simulated temporal-zonal cross section of eddy kinectic energy (EKE) difference (unit: m^2/s^2) due to LST and SUBT effect at 150 hPa and averaged over 25° N–35° N. **b** Is same as **a** but for geopotential height (unit: m^2/s^2)

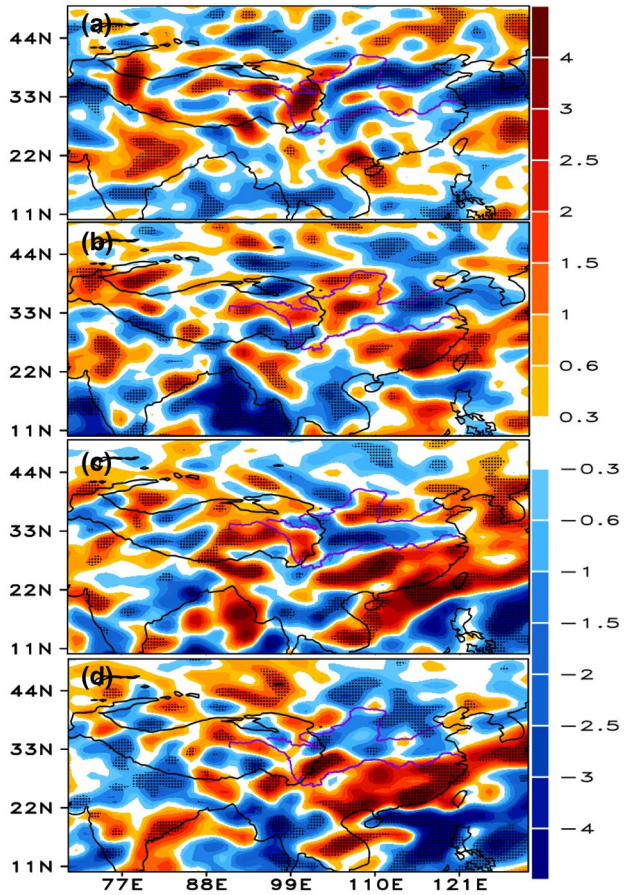

Fig. 11 Same as Fig. 10 but for 150 hPa wind divergence (units: 10–6 /s)

summer extreme hydroclimatic events, such as droughts, floods, and heatwaves in East Asia and South Asia. After a deeper and comprehensive investigations for the 1998 case, the 2003 case shows a very consistent mechanisms with the 1998 case but with an opposite sign due to the cold TP spring LST and SUBT in 2003 (e.g., Figs. 7a, b vs. 14a, b).

4 Summary and conclusions

Recent observational and modeling studies have demonstrated the significant influence of the Tibetan Plateau springtime LST and SUBT on downstream summer droughts/floods events in East Asia, highlighting the potential application of LST and SUBT on sub-seasonal to seasonal prediction. The East Asian summer monsoon rainfall has profound impacts on population wellbeing and agriculture as well as the economy of the region. Using the GFS/SSiB2, in this study, we investigated the potential impact of the spring land surface temperature anomaly over the Tibetan Plateau on summer rainfall flood/drought events in the East Asian continent with another case study: 1998 flooding in the Yangtze River Basin. The June 1998 was characterized by a disastrous flood over the southern Yangtze River Basin area in East Asia and below normal rainfall to the north, whilst in spring was observed an above normal (warm) land surface temperature anomaly over the Tibetan Plateau.

Our modeling experiments indicate that the warm spring land surface temperature anomaly over the Tibetan Plateau may contribute to the June 1998 downstream extreme flooding in the lowland plain in Eastern China. Results from both Cases 1998 and 2003 have shown that the warm/cold spring land surface temperature anomaly is able to explain an important amount of rainfall variance at seasonal and intra-seasonal variability, indicating the importance of land–atmosphere interactions across the Tibetan Plateau for more skillful S2S prediction across East Asia. Enlightened by some preliminary evidence (Xue et al. 2021), we have demonstrated that the warm/cold springtime Tibetan Plateau 2m-temperature anomaly has a much larger scale remote effect on summer rainfall anomaly with different hot spots identified over the Asian continent (see Figs. 6c, d and 13c, d).

The imposed warm LST and SUBT anomaly strengthens the Tibetan Plateau diabatic heating and the perturbation propagates eastward along the upper-level westerly jet, which in turn interact with the SAH and the upward motion, promoting an increase of the atmospheric baroclinic instability driving a stronger moisture flux convergence over the south of YRB, thereby leading to heavy rainfall in the downstream region of East Asia. The simulation results provide further evidence of the great importance of the Tibetan Plateau spring land surface temperature anomaly in regulating summer extreme hydroclimatic events, such as droughts, and floods in both East Asia and South Asia.

The results presented in this paper propose a new perspective for understanding the possible physical mechanisms of LST and SUBT effects in East Asia. While our results are based on a single model and two cases (1998 and 2003), more models and cases with different initial conditions should be considered. Thus we plan to use more models from the LS4P phase I (LS4P-I) simulations (Xue et al. 2021) to further assess the robustness of our conclusions. The potential impact of spin-up time on the relationship between spring TP LST/SUBT anomalies and downstream rainfall anomalies in South-East Asia will also be investigated. Likewise, LS4P-I multi-model inter-comparison project will provide valuable platforms to identify the SST possible contribution in these extreme events. It is important to note that previous LST and SUBT studies (Xue et al. 2012, 2016a, 2018; Diallo et al 2019) suggested that high-resolution state-of-the-art regional

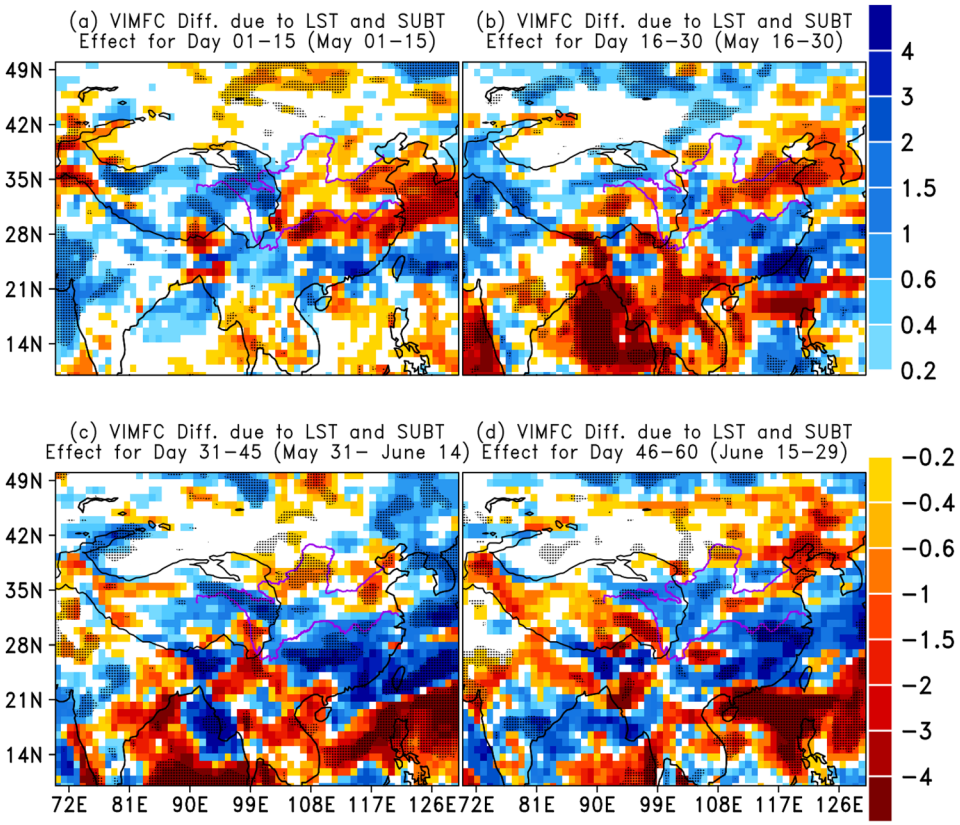

Fig. 12 Vertical integrated moisture flux convergence (VIMFC) (unit: mm/day) difference due to LST and SUBT effects. **a** Day 1–15 (May 1st–May 15th 1998); **b** Day 16–30 (May 16th–May 30th 1998); **c** Day 31–45 (May 31st–June 14th 1998); **d** Day 46–60 (June 15th–June 29th 1998). The dotted regions denote/highlight the statistical significance at the $\alpha < 0.05$ level of two-tailed t-test values

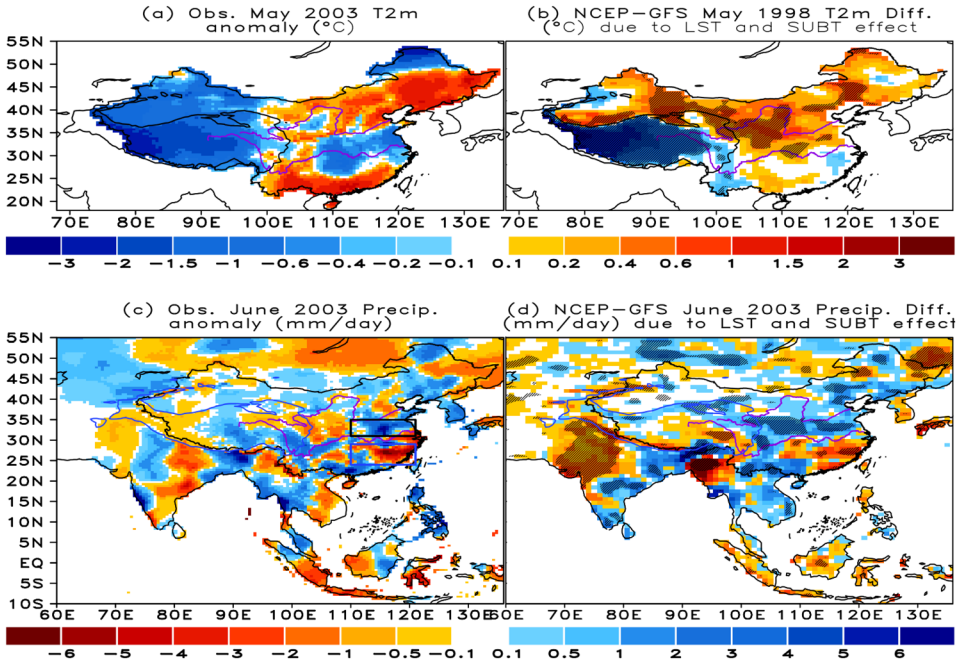

Fig. 13 Observed and simulated May 2003 2m-temperature anomalies (°C). **a** Observed May 2m-temperature difference between 2003 and the climatology reference (1981–2010); **b** GFS/SSiB2 simulated 2m-temperature difference due to LST and SUBT effect. **c, d** Same as **a, b** but for June 2003 rainfall anomalies (mm/day). Blue (black) box in **c** denotes the south (north) of Yangtze River Basin used for the rainfall regional averages. The dotted regions denote the statistical significance at the $\alpha < 0.05$ level of two-tailed t-test values

climate model, simulates better downstream rainfall anomaly and associated mechanisms of LST and SUBT effects in North America. Therefore, it is recommended to dynamically downscale LS4P-I models to quantify downstream rainfall anomalies uncertainties before investigating the physical mechanisms.

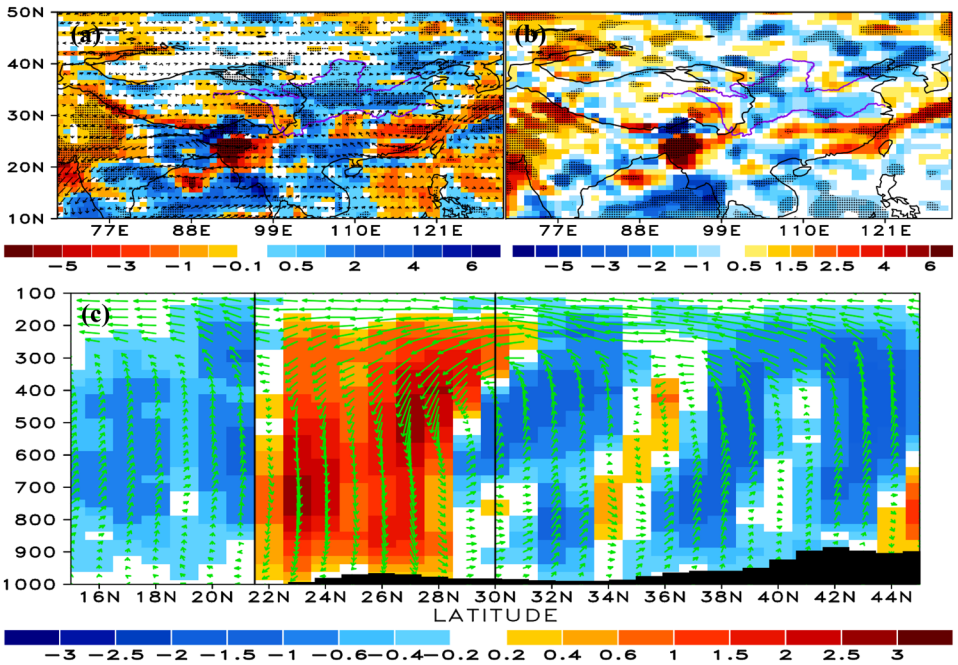

Fig. 14 Simulated June 2003 differences due to LST and SUBT effect for: **a** Vertical integrated (1000–300 hPa) moisture flux transport (vector, kg/m/s) and the corresponding moisture flux convergence (shading, mm/day); **b** 500 hPa Vertical velocity (unit: 10^{-2} Pa/s); **c** the pressure-longitude cross sections of vertical vectors (vectors, v and − 50xw, unit: 10^{-2} Pa/s) and Vertical velocity (shading, unit: 10^{-2} Pa/s) averaged from 110° E to 121° E. The black shaded areas in **c** indicate grid points under the topography, while the two blacks vertical lines delineate the south of YRB region

Supplementary Information The online version contains supplementary material available at https://doi.org/10.1007/s00382-021-06053-8.

Acknowledgements This study was supported by a grant from the U.S. National Science Foundation (Grant No AGS-1849654). The authors would like to thank the Texas Advanced Computing Center (TACC) at the University of Texas at Austin for providing invaluable computer time for the model simulations, as well as the anonymous reviewers' and the editor for providing very constructive comments/suggestions to help improve the paper. All the model runs described in this study were carried out at the TACC stampede 2. All simulations datasets analyzed in this study are archived in the Department of Geography at the University of California—Los Angeles and can be obtained upon request by contacting the corresponding author (idiallo.work@gmail.com or ismailladiallo@gmail.com).

Funding The U.S. National Science Foundation (Grant No AGS-1849654).

Declarations

Conflict of interest All authors declare that there are no conflicts of interest.

Availability of data and material The reference datasets are downloaded from open sources. The gridded observational datasets (CMA) are available from http://data.cma.cn/site/index.html (http://data.cma.cn/en; for English). All simulations datasets and processed datasets are available upon request from the corresponding author (ismailladiallo@gmail.com or idiallo.work@gmail.com).

Code availability All analysis code is available upon request from the corresponding author (ismailladiallo@gmail.com or idiallo.work@gmail.com).

References

Anwar SA, Diallo I (2021) Modelling the Tropical African Climate using a state-of-the-art coupled regional climate-vegetation model. Clim Dyn. https://doi.org/10.1007/s00382-021-05892-9

Arakawa A, Schubert WH (1974) Interaction of a cumulus cloud ensemble with the large scale environment. Part I. J Atmos Sci 31:674–701

Ashfaq M (2020) Topographic controls on the distribution of summer monsoon precipitation over South Asia. Earth Syst Environ 4:667–683. https://doi.org/10.1007/s41748-020-00196-0

Bamba A, Diallo I et al (2018) Effect of the African greenbelt position on West African summer climate: a regional climate modeling study. Theor Appl Climatol 137(1–2):309–322. https://doi.org/10.1007/s00704-018-2589-z

Bamzai A, Shukla J (1999) Relation between Eurasian snow cover, snow depth and the Indian summer monsoon: an observational study. J Clim 12:3117–3132. https://doi.org/10.1175/1520-0442(1999)012%3c3117:RBESCS%3e2.0.CO;2

Bao Q, Yang J, Liu Y, Wu G, Wang B (2010) Roles of anomalous Tibetan Plateau warming on the severe 2008 winter storm in central-southern China. Mon Weather Rev 138:2375–2384. https://doi.org/10.1175/2009MWR2950.1

Chen D, Sun JQ, Gao Y (2019) Distinct impact of the Pacific multi-decadal oscillation on precipitation in Northeast China during April in different Pacific multi-decadal oscillation phases. Int J Climatol. https://doi.org/10.1002/joc.6291

China Meteorological Administration [CMA] (1999) National weather and climate review and impact assessment. China meteorological yearbook. Meteorological Press, Beijing, pp 257–274

Choi YW, Ahn JB (2019) Possible mechanisms for the coupling between late spring sea surface temperature anomalies over tropical Atlantic and East Asian summer monsoon. Clim Dyn 53:6995–7009

Chow KC, Chan JCL, Shi X, Liu Y, Ding Y (2008) Time-lagged effects of spring Tibetan Plateau soil moisture on the monsoon over China in early summer. Int J Climatol 28:55–67

Chun H-Y, Baik J-J (1998) Momentum flux by thermally induced internal gravity waves and its approximation for large-scale models. J Atmos Sci 55:3299–3310

Clough SA, Shephard MW, Mlawer E, Delamere JS, Iacono M, Cady-Pereira K, Boukabara S, Brown PD (2005) Atmospheric radiative transfer modeling: a summary of the AER codes. J Quant Spectrosc Radiat Trans 91:233–244

CMA (2004) National weather and climate review and impact assessment. China meteorological yearbook. Meteorological Press, Beijing, pp 446–467 (**In Chinese**)

Deng X, Sun Z (1994) Characteristics of temporal evolution of northern storm tracks (in Chinese). J Nanjing Inst Meteorol 17(2):165–170. https://doi.org/10.13878/j.cnki.dqkxxb.1994.02.006

Dey B, Kumar OSRUB (1983) An apparent relationship between Eurasian snow cover and the advanced period of the Indian summer monsoon. J Appl Meteorol 21:1929–1932. https://doi.org/10.1175/1520-0450(1982)021%3c1929:AARBES%3e2.0.CO;2

Diallo I, Giorgi F, Sukumaran S, Stordal F, Giuliani G (2015) Evaluation of RegCM4 driven by CAM4 over Southern Africa: mean climatology, interannual variability and daily extremes of wet season temperature and precipitation. Theor Appl Climatol 121(3–4):749–766

Diallo I, Giorgi F, Stordal F (2018) Influence of Lake Malawi on regional climate from a double-nested regional climate model experiment. Clim Dyn 50(9–10):3397–3411. https://doi.org/10.1007/sOO382-017-3811-x

Diallo I, Xue Y, Li Q et al (2019) Dynamical downscaling the impact of spring Western US land surface temperature on the 2015 flood extremes at the Southern Great Plains: effect of domain choice, dynamic cores and land surface parameterization. Clim Dyn 53:1039–1061. https://doi.org/10.1007/s00382-019-04630-6

Dickinson RE (1988) The force-restore model for surface temperatures and its generalizations. J Clim 1:1086–1097. https://doi.org/10.1175/1520-0442(1988)001%3c1086:TFMFST%3e2.0.CO;2

Ding R, Ha KJ, Li J (2010) Interdecadal shift in the relationship between the East Asian summer monsoon and the tropical Indian Ocean. Clim Dyn 34:1059–1071. https://doi.org/10.1007/s00382-009-0555-2

Duan AM, Wu GX (2005) Role of the Tibetan Plateau thermal forcing in the summer climate patterns over subtropical Asia. Clim Dyn 24:793–807

Duan AM, Li F, Wang MR, Wu GX (2011) Persistent weakening trend in the spring sensible heat source over the Tibetan Plateau and its impact on the Asian summer monsoon. J Clim 24:5671–5682

Fan Y, van den Dool H (2008) A global monthly land surface air temperature analysis for 1948–present. J Geophys Res 113:D01103

Fasullo J (2004) A stratified diagnosis of the Indian Monsoon-Eurasian snow cover relationship. J Clim 17:1110–1122. https://doi.org/10.1175/1520-0442(2004)017%3c1110:ASDOTI%3e2.0.CO;2

Gao C, Li G, Bei X, Li X (2020) Effect of spring soil moisture over the Indo-China Peninsula on the following summer extreme precipitation events over the Yangtze River basin. Clim Dyn 45:3845–3861

Ge J, You Q, Zhang Y (2019) Effect of Tibetan Plateau heating on summer extreme precipitation in eastern China. Atmos Res 218:364–371

Gelaro R, McCarty W, Suàrez MJ et al (2017) The modern-era retrospective analysis for research and applications, version 2 (MERRA-2). J Clim 30(14):5419–5454. https://doi.org/10.1175/JCLI-D-16-0758.1

Good EJ, Ghent DJ, Bulgin CE, Remedios JJ (2017) A spatiotemporal analysis of the relationship between near-surface air temperature and satellite land surface temperatures using 17 years of data from the ATSR series. J Geophys Res Atmos 122(17):9185–9210. https://doi.org/10.1002/2017JD026880

Han S, Shi CX, Xu B et al (2019) Development and evaluation of hourly and kilometer resolution retrospective and real-time surface meteorological blended forcing dataset (SMBFD) in China. J Meteorol Res 33:1168–1181. https://doi.org/10.1007/s13351-019-9042-9

Harris I, Osborn TJ, Jones PD, Lister DH (2020) Version 4 of the CRU TS monthly high-resolution gridded multivariate climate dataset. Sci Data 7:109

Hertwig E, von Storch J-S, Handorf D, Dethloff K, Fast I, Krismer T (2015) Effect of horizontal resolution on ECHAM6-AMIP performance. Clim Dyn 45:185–211. https://doi.org/10.1007/s00382-014-2396-x

Hong SY, Pan HL (1996) Non-local boundary layer vertical diffusion in a medium range forecast model. Mon Weather Rev 124:2322–2339

Hong SY, Pan HL (1998) Convective trigger function for a mass-flux cumulus parameterization scheme. Mon Weather Rev 126:2599–2620

Hoskins B (1991) Toward a PV-h view of the general circulation. Tellus 43:27–35

Hoskins BJ, Ambrizzi T (1993) Rossby wave propagation on a realistic longitudinaly varying flow. J Atmos Sci 50:1661–1671

Hoskins BJ, Valdes PJ (1990) On the existence of storm-tracks. J Atmos Sci 47:1854–1864. https://doi.org/10.1175/1520-0469(1990)047%3c1854:OTEOST%3e2.0.CO;2

Hsu HH, Liu X (2003) Relationship between the Tibetan Plateau heating and East Asian summer monsoon rainfall. Geophys Res Lett 30(20):2066. https://doi.org/10.1029/2003GL017909

Hu Q, Feng S (2004) A role of the soil enthalpy in land memory. J Clim 17(18):3633–3643

Huang RH, Sun FY (1992) Impact of the tropical western Pacific on the East Asian summer monsoon. J Meteorol Soc Jpn 70:243–256

Huang RH, Xu YH, Wang PF (1998) The features of the particularly severe flood over the Changjiang (Yangtze River) basin during the summer of 1998 and exploration of its causes. Clim Environ Res 3:300–313 (**In Chinese**)

Huang RH, Chen JL, Huang G (2007) Characteristics and variations of the East Asian monsoon system and its impacts on climate disasters in China. Adv Atmos Sci 24:993–1023

Huang H, Xue Y, Chilukoti N, Liu Y, Chen G, Diallo I (2020) Assessing global and regional effects of reconstructed land use and land cover change on climate since 1950 using a coupled land-atmosphere-ocean model. J Clim 33:8997–9013. https://doi.org/10.1175/JCLI-D-20-0108.1

Jiang DB, Ding ZL, Drange H, Gao YQ (2008a) Sensitivity of East Asian climate to the progressive uplift and expansion of the Tibetan Plateau under the Mid-Pliocene boundary conditions. Adv Atmos Sci 25(5):709–722. https://doi.org/10.1007/s00376-008-0709-x

Jiang T, Kundzewicz ZW, Su B (2008b) Changes in monthly precipitation and flood hazard in the Yangtze River basin, China. Int J Climatol 28:1471–1481. https://doi.org/10.1002/joc.1635

Kalnay E, Kanamitsu M, Kistler R, Collins W, Deaven D, Gandin L, Iredell M, Saha S, White G, Woollen J, Zhu Y, Leetmaa A, Reynolds R, Chelliah M, Ebisuzaki W, Higgins W, Janowiak J, Mo KC, Ropelewski C, Wang J, Jenne R, Joseph D (1996) The NCEP/NCAR 40-year reanalysis project. Bull Am Meteorol Soc 77:437–471. https://doi.org/10.1175/1520-0477(1996)077%3C0437:TNYRP%3E2.0.CO;2

Kanamitsu M, Ebisuzaki W, Woollen J, Yang SK, Hnilo JJ, Fiorino M, Potter GL (2002) NCEP-DOE AMIP-II reanalysis (R-2). Bull Am Meteorol Soc 83:1631–1643

Koster RD, Dirmeyer PA, Guo Z, Bonan G, Chan E, Cox P, Gordon CT, Kanae S, Kowalczyk E, Lawrence D, Liu P, Lu CH, Malyshev S,

McAvaney B, Mitchell K, Mocko D, Oki T, Oleson K, Pitman A, Sud YC, Taylor CM, Verseghy D, Vasic R, Xue Y, Yamada T (2004) Regions of strong coupling between soil moisture and precipitation. Science 305:1138–1140

Kripalani RH, Kulkarni A, Sabade SS (2003) Western Himalayan snow cover and Indian monsoon rainfall: a re-examination with INSAT and NCEP/NCAR data. Theor Appl Climatol 74:1–18. https://doi.org/10.1007/s00704-002-0699-z

Lau KM (1992) East Asian summer monsoon rainfall variability and climate teleconnection. J Meteor Soc Jpn 70:211–240

Lau K, Weng H (2001) Coherent modes of global SST and summer rainfall over China: an assessment of the regional impacts of the 1997 98 El Nin˜o. J Clim 14:1294–1308. https://doi.org/10.1175/1520-0442(2001)014\1294:CMOGSA[2.0.CO;2

Lee S, Lee M-I (2019) Effects of surface vegetation on the intensity of East Asian summer monsoon as revealed by observation and model experiments. Int J Climatol. https://doi.org/10.1002/joc.6420

Lee S, Lee M-I (2020) Effects of surface vegetation on the intensity of East Asian summer monsoon as revealed by observation and model experiments. Int J Climatol 40:3634–3648. https://doi.org/10.1002/joc.6420

Lee J, Xue Y, De Sales F et al (2019) Evaluation of multi-decadal UCLA-CFSv2 simulation and impact of interactive atmospheric-ocean feedback on global and regional variability. Clim Dyn 52:3683–3707. https://doi.org/10.1007/s00382-018-4351-8

Li C, Yanai M (1996) The onset and interannual variability of the Asian summer monsoon in relation to land–sea thermal contrast. J Clim 9:358–375

Li H, Dai A, Zhou T, Lu J (2010) Responses of East Asian summer monsoon to historical SST and atmospheric forcing during 1950–2000. Clim Dyn 34(4):501–514

Lin R, Zhu J, Zheng F (2016) Decadal shifts of East Asian summer monsoon in a climate model free of explicit GHGs and aerosols. Sci Rep 6:38546. https://doi.org/10.1038/srep38546

Liu XD, Yin ZY (2002) Sensitivity of East Asian monsoon climate to the uplift of the Tibetan Plateau. Palaeogeogr Palaeoclimatol Palaeoecol 183(3–4):223–245

Liu YM, Wu GX, Hong JL, Dong BW, Duan AM, Bao Q, Zhou LJ (2012) Revisiting Asian monsoon formation and changes associated with Tibetan Plateau forcing: II. Change. Clim Dyn. https://doi.org/10.1007/s00382-012-1335-y

Liu Y, Xue Y, Li Q, Lettenmaier D, Zhao P (2020) Investigation of the variability of near-surface temperature anomaly and its causes over the Tibetan Plateau. J Geophys Res Atmos 125:650. https://doi.org/10.1029/2020jd032800

Lu R (2000) Anomalies in the tropics associated with the heavy rainfall in East Asia during the summer of 1998. Adv Atmos Sci 17(2):205–220

Ministry of Water Resources of China (1999) China's 98 Great Flood. China Water Resources Yearbook. China Water Resources and Hydropower Press, Beijing, pp 518–523

Mlawer EJ, Taubman SJ, Brown PD, Iacono MJ, Clough SA (1997) Radiative transfer for inhomogeneous atmospheres: RRTM, a validated correlated-k model for the longwave. J Geophys Res Atmos 102:16663–16682

Moorthi S, Pan HL, Caplan P (2001) Changes to the 2001 NCEP operational MRF/AVN global analysis/forecast system. NWS Tech Proc Bull 484:1–14

Nitta T (1987) Convective activities in the tropical western Pacific and their impact on the Northern Hemisphere summer circulation. J Meteorol Soc Jpn 65:373–390

Notaro M, Chen GS, Liu Z (2011) Vegetation feedbacks to climate in the global monsoon regions. J Clim. https://doi.org/10.1175/2011JCLI4237.1

Pan H-L, Wu W-S (1995) Implementing a mass flux convective parameterization package for the NMC medium-range forecast model. In: NMC Office Note 409, NCEP/EMC, Camp Springs, Md, p 40

Pincus R, Barker HW, Morcrette JJ (2003) A fast, flexible, approximate technique for computing radiative transfer in inhomogeneous cloud fields. J Geophys Res 108:4376

Ren X, Yang D, Yang X-Q (2015a) Characteristics and mechanisms of the subseasonal eastward extension of the South Asian High. J Clim 28(17):6799–6822

Ren Z, Zhang M, Wang S, Qiang F, Zhu X, Dong L (2015b) Changes in daily extreme precipitation events in South China from 1961 to 2011. J Geogr Sci 25:58–68. https://doi.org/10.1007/s11442-015-1153-3

Saha S, Moorthi S, Pan HL, Wu X, Wang J, Nadiga S, Tripp P, Kistler R, Woollen J, Behringer D, Liu H (2010) The NCEP climate forecast system reanalysis. Bull Am Meteorol Soc 91:1015–1057. https://doi.org/10.1175/2010BAMS3001.1

Saha S, Moorthi S, Wu X, Wang J, Nadiga S, Tripp P, Behringer D, Hou YT, Chuang HY, Iredell M, Ek M (2014) The NCEP climate forecast system version 2. J Clim 27:2185–2208. https://doi.org/10.1175/JCLI-D-12-00823.1

Sampe T, Xie SP (2010) Large-scale dynamics of the Meiyu-Baiu rainband: environmental forcing by the westerly jet. J Clim 23:113–134

Sellers PJ, Randall DA, Collatz GJ, Berry JA, Field CB, Dazlich DA, Zhang C, Colello GD, Bounoua L (1996) A revised land surface parametrization (SiB2) for atmospheric GCMs. Part I: model formulation. J Clim 9:676–705

Seol KH, Hong SY (2009) Relationship between the Tibetan Snow in spring and the East Asian summer monsoon in 2003: a global and regional modeling study. J Clim 22:2095–2110

Shen H, He S, Wang H (2019) Effect of summer Arctic sea ice on the reverse August precipitation anomaly in Eastern China between 1998 and 2016. J Clim 32:3389–3407

Skamarock WC, Klemp JB, Dudhia J, Gill D, Barker D, Duda M, Huang X, Wang W, Powers J (2008) A description of the advanced research WRF version 3. In: NCAR technical note, NCAR/TN-475?STR, p 125

Song F, Zhou T (2014) The climatology and inter-annual variability of East Asian summer monsoon in CMIP5 coupled models: does air-sea coupling improve the simulations? J Clim 27:8761–8777. https://doi.org/10.1175/JCLI-D-14-00396.1

Song F, Zhou T (2015) The crucial role of internal variability in modulating the decadal variation of the east Asian summer monsoon–ENSO relationship during the twentieth Century. J Clim 28:7093–7107. https://doi.org/10.1175/jcli-d-14-00783.1

Takaya Y, Ishikawa I, Kobayashi C, Endo H, Ose T (2020) Enhanced Meiyu-Baiu rainfall in Early Summer 2020: aftermath of the 2019 super IOD event. Geophys Res Lett 47(22):e2020GL090671

Tian S-F, Yasunari T (1992) Time and space structure of interannual variations in summer rainfall over China. J Meteorol Soc Jpn 70:585–596

Ullah W, Guojie W, Gao Z et al (2021) Observed linkage between Tibetan Plateau soil moisture and South Asian summer precipitation and the possible mechanism. J Clim 34(1):361–377

Vallis GK, Gerber EP (2008) Local and hemispheric dynamics of the North Atlantic oscillation, annular patterns and the zonal index. Dyn Atmos Oceans 44:184–212

Wallace JM, Lim GH, Blackmon ML (1988) Relationship between cyclone tracks, anticyclone tracks and baroclinic waveguides. J Atmos Sci 45:439–462

Wan BC, Gao ZQ, Chen F, Lu CG (2017) Impact of Tibetan Plateau surface heating on persistent extreme precipitation events

in Southeastern China. Mon Weather Rev 145(9):3485–3505. https://doi.org/10.1175/Mwr-D-17-0061.1
Wang B (ed) (2006) The Asian monsoon. Springer, Berlin
Wang B, Wu R, Fu X (2000) Pacific-East Asian teleconnection: how does ENSO affect East Asian climate? J Clim 13:1517–1536. https://doi.org/10.1175/1520-0442(2000)013\1517:PEATHD[2.0.CO;2
Wang Y, Zhai P, Tian H (2006) Characteristics of high temperature variation in southern China in recent 40 years and high temperature events in 2003. Meteorol Mon 10:27–33 (**In Chinese**)
Wang B, Bao Q, Hoskins B, Wu G, Liu Y (2008) Tibetan Plateau warming and precipitation changes in East Asia. Geophys Res Lett 35:L14702. https://doi.org/10.1029/2008GL034330
Wang Z, Duan A, Wu G (2014) Time-lagged impact of spring sensible heat over the Tibetan Plateau on the summer rainfall anomaly in East China: case studies using the WRF model. Clim Dyn 42:2885–2898
Wang PX, Wang B, Cheng H et al (2017) The global monsoon across time scales: mechanisms and outstanding issues. Earth Sci Rev 174:84–121
Wu J, Gao X (2013) A gridded daily observation dataset over China region and comparison with the other datasets. Chin J Geophy 56:1102–1111 (**In Chinese**)
Wu G, Liu Y (2016) Impacts of the Tibetan Plateau on Asian climate. Meteorol Monogr 56:7–1
Wu TW, Qian ZA (2003) The relationship between the Tibetan winter snow and the Asian summer monsoon and rainfall: an observational investigation. J Clim 16:2038–2051. https://doi.org/10.1175/1520-0442(2003)016\2038:TRBTTW[2.0.CO;2
Wu R, Hu Z, Kirtman B (2003) Evolution of ENSO-related rainfall anomalies in East Asia. J Clim 16(22):3742–3758. https://doi.org/10.1175/1520-0442(2003)016\3742:EOERAI[2.0.CO;2
Wu Z, Wang B, Li J, Jin FF (2009) An empirical seasonal prediction model of the east Asian summer monsoon using ENSO and NAO. J Geophys Res 114:D18120. https://doi.org/10.1029/2009jd011733
Wu GX, Liu YM, He B, Bao Q, Duan AM, Jin FF (2012) Thermal controls on the Asian summer monsoon. Sci Rep 2:404
Xiao Z, Duan A (2016) Impacts of Tibetan Plateau snow cover on the interannual variability of the East Asian summer monsoon. J Clim 29:8495–8514
Xu Z, Fan K, Wang H (2015) Decadal variation of summer precipitation over china and associated atmospheric circulation after the late 1990s. J Clim 28:4086–4106
Xue Y, Sellers PJ, Kinter JL, Shukla J (1991) A simplified biosphere model for global climate studies. J Clim 4(3):345–364
Xue Y, Juang HM, Li W, Prince S, DeFries R, Jiao Y, Vasic R (2004) Role of land surface processes in monsoon development: East Asia and West Africa. J Geophys Res 109:D03105. https://doi.org/10.1029/2003JD003556
Xue Y, De Sales F, Vasic R, Mechoso CR, Arakawa A, Prince S (2010) Global and seasonal assessment of interactions between climate and vegetation biophysical processes: a GCM study with different land-vegetation representations. J Clim 23:1411–1433
Xue Y, Vasic R, Janjic Z, Liu YM, Chu PC (2012) The impact of spring subsurface soil temperature anomaly in the western US on North American summer precipitation: a case study using regional climate model downscaling. J Geophys Res Atmos 117(D11):D11103
Xue Y, Oaida CM, Diallo I, Neelin JD, Li S, De Sales F, Gu Y, Robinson D, Vasic R, Yi L (2016a) Spring land temperature anomalies in northwestern US and the summer drought over Southern Plains and adjacent areas. Environ Res Lett 11:044018. https://doi.org/10.1088/1748-9326/11/4/044018
Xue Y, De Sales F, Lau WKM, Boone A, Kim KM, Mechoso CR, Wang G, Kucharski F, Schiro K, Hosaka M, Li S, Druyan LM, Sanda IS, Thiaw W, Zeng N, Comer RE, Lim YK, Mahanama S, Song G, Gu Y, Hagos SM, Chin M, Schubert S, Dirmeyer P, Leung LR, Kalnay E, Kitoh A, Lu CH, Mahowald NM, Zhang Z (2016b) West African monsoon decadal variability and surface-related forcings: second West African Monsoon Modeling and Evaluation Project Experiment (WAMME II). Clim Dyn 47:3517–3545
Xue Y, Diallo I, Li W, Neelin JD, Chu P-C, Vasic R, Guo W, Li Q, Robinson DA, Zhu Y, Fu C, Oaida CM (2018) Spring land surface and subsurface temperature anomalies and subsequent downstream late spring-summer droughts/floods in North America and East Asia. J Geophys Res Atmos. https://doi.org/10.1029/2017JD028246
Xue Y, Yao T, Boone AA, Diallo I et al (2021) Impact of initialized land surface temperature and snowpack on subseasonal to seasonal prediction project, phase I (LS4P-I): organization and experimental design. Geosci Model Dev 14:4465–4494. https://doi.org/10.5194/gmd-14-4465-2021
Yanai M, Wu GX (2006) Effects of the Tibetan Plateau. In: Wang B (ed) The Asian Monsoon. Springer, New York, pp 513–549. https://doi.org/10.1007/3-540-37722-0_13
Yao T et al (2019) Recent third pole's rapid warming accompanies cryospheric melt and water cycle intensification and interactions between monsoon and environment: multi-disciplinary approach with observation, modeling and analysis. Bull Am Meteorol Soc 100(3):423–444. https://doi.org/10.1175/bams-d-17-0057.1
Yasunari T, Miwa T (2006) Convective cloud systems over the Tibetan Plateau and their impact on meso-scale disturbances in the Meiyu/Baiu frontal zone: a case study in 1998. J Meteor Soc Jpn 84:783–803
You QL, Min J, Zhang W, Pepin N, Kang S (2015) Comparison of multiple datasets with gridded precipitation observations over the Tibetan Plateau. Clim Dyn 45(3):791–806. https://doi.org/10.1007/s00382-014-2310-6
Yu L, Xue Y, Diallo I (2021) Vegetation greening in China and its effect on summer regional climate. Sci Bull 66(1):13–17. https://doi.org/10.1016/j.scib.2020.09.003
Zhan XW, Xue YK, Collatz GJ (2003) An analytical approach for estimating CO_2 and heat fluxes over the Amazonian region. Ecol Model 162:97–117
Zhang L, Zhou T (2015) Drought over East Asia: a review. J Clim 28(8):150203142724009
Zhang Q, Zhao Y, Fan S (2016) Development of hourly precipitation datasets for national meteorological stations in China. Torrential Rain Disasters 35(2):182–186
Zhao Q, Carr FH (1997) A prognostic cloud scheme for operational NWP models. Mon Weather Rev 125:1931–1953
Zhao TB, Fu CB (2006) Preliminary comparison and analysis between ERA-40, NCEP-2 reanalysis and observations over China. Clim Environ Res 11:14–32. https://doi.org/10.3969/jissn.1006-9585.2006.01.002.(inChinese)
Zhao P, Zhang X, Zhou X, Ikeda M, Yin Y (2004) The sea ice extent anomaly in the North Pacific and its impact on the East Asian summer monsoon rainfall. J Clim 17:3434–3447. https://doi.org/10.1175/1520-0442(2004)017%3c3434:TSIEAI%3e2.0.CO;2
Zheng F, Li J, Li Y, Zhao S, Deng D (2016) Influence of the summer NAO on the spring-NAO-based predictability of the East Asian summer monsoon. J Appl Meteorol Climatol 55:1459–1476
Zhisheng A, Kutzbach JE, Prell WL, Porter S (2001) Evolution of Asian monsoons and phased uplift of the Himalaya-Tibetan plateau since Late Miocene times. Nature 411:62–66. https://doi.org/10.1038/35075035
Zhou ZQ, Xie SP, Zhang RH (2021) Historic Yangtze flooding of 2020 tied to extreme Indian Ocean conditions. Proc Natl Acad Sci 118:2022255118. https://doi.org/10.1073/pnas.2022255118
Zhu W, Sun ZB (2000) Impacts of Kuroshio SSTA on storm track over North Pacific in winter. Q J Appl Meteor 11:145–153

Zuo Z, Yang S, Zhang R, Jiang P, Zhang L, Wang F (2013) Long-term variations of broad-scale Asian summer monsoon circulation and possible causes. J Clim 26:8947–8961